

# OPERATING INSTRUCTIONS AND SYSTEM DESCRIPTION OF THE

## SEC-03M

# SINGLE ELECTRODE CLAMP AMPLIFIER MODULE FOR EPMS SYSTEMS



VERSION 1.8  
npi 2014

## Table of Contents

About this Manual .....	4
1. Safety Regulations .....	5
2. EPMS-07 Modular Plug-In System .....	6
2.1. General System Description / Operation .....	6
2.2. EPMS-07 Housing .....	6
2.3. EPMS-E-07 Housing .....	6
2.4. PWR-03D .....	6
2.5. System Grounding .....	7
EPMS-07 .....	7
EPMS-E-07 .....	7
2.6. Technical Data .....	7
EPMS-07 .....	7
EPMS-E-07 .....	7
3. Introduction .....	8
3.1. Why a Single Electrode Clamp? .....	8
3.2. Principle of Operation .....	10
Major Advantages of the npi SEC System .....	12
3.3. Advantages of the Modular SEC-03M System .....	12
4. SEC-03M System .....	13
4.1. SEC-03M Components .....	13
4.2. Description of the Front Panel .....	14
5. Headstages .....	19
5.1. Standard and low-noise (SEC-HSP) headstages .....	19
5.2. Low-noise headstage (SEC-HSP) .....	21
6. Setting up the SEC-03M System .....	22
7. Passive Cell Model .....	23
7.1. Cell Model Description .....	23
7.2. Connections and Operation .....	24
7.3. Connections and Operation .....	25
8. Test and Tuning Procedures .....	27
8.1. Headstage Bias Current Adjustment .....	27
8.2. Electrode Selection .....	28
8.3. Offset Compensation .....	28
8.4. Bridge Balance (in BR mode) .....	29
8.5. Switching Frequency and Capacitance Compensation (in switched modes) .....	31
Criteria for the selection of the switching frequency .....	31
8.6. Capacity Compensation - Tuning Procedure .....	33
First part: basic setting .....	33
Second part: fine tuning .....	38
8.7. Testing Operation Modes .....	39
Current Clamp (in BR- or discontinuous CC mode) .....	39
Voltage Clamp .....	39
9. Sample Experiments .....	41
9.1. Sample Experiment using a Sharp Microelectrode .....	41
9.2. Sample Experiment using a Suction Electrode .....	44
10. Tuning VC Performance .....	46
General Considerations .....	46
Tuning Procedure .....	47
11. Trouble Shooting .....	48
12. Appendix .....	49

12.1. Theory of Operation .....	49
12.2. Speed of Response of SEC Single Electrode Clamps .....	50
12.3. Tuning Procedures for VC Controllers.....	50
Practical Implications .....	51
13. Literature about npj single electrode clamp amplifiers .....	53
13.1. Paper in Journals.....	53
13.2. Books.....	64
14. SEC-03M Specifications – Technical Data.....	65
15. Index .....	68

## About this Manual

This manual should help to setup and use SEC systems correctly and to perform reliable experiments.

If you are not familiar with the use of instruments for intracellular recording of electrical signals please read the manual completely. The experienced user should read at least chapters 1, 4, 8 and 10.

**Important:** Please read chapter 1 carefully! It contains general information about the safety regulations and how to handle highly sensitive electronic instruments.

### Signs and conventions

In this manual all elements of the front panel are written in capital letters as they appear on the front panel.

System components that are shipped in the standard configuration are marked with ✓, optional components with ⇄. In some chapters the user is guided step by step through a certain procedure. These steps are marked with □.

Important information and special precautions are highlighted in gray.

### Abbreviations

$C_m$ : cell membrane capacitance

$C_{stray}$ : electrode stray capacitance

GND: ground

$I_{max}$ : maximal current

$R_a$ : access resistance

$R_m$ : cell membrane resistance

$R_{EL}$ : electrode resistance

SwF: switching frequency

$\tau_{Cm}$ : time constant of the cell membrane

$V_{REL}$ : potential drop at  $R_{EL}$

## 1. Safety Regulations

**VERY IMPORTANT:** Instruments and components supplied by npi electronic are NOT intended for clinical use or medical purposes (e.g. for diagnosis or treatment of humans), or for any other life-supporting system. npi electronic disclaims any warranties for such purpose. Equipment supplied by npi electronic must be operated only by selected, trained and adequately instructed personnel. For details please consult the **GENERAL TERMS OF DELIVERY AND CONDITIONS OF BUSINESS** of npi electronic, D-71732 Tamm, Germany.

- 1) **GENERAL:** This system is designed for use in scientific laboratories and must be operated only by trained staff. General safety regulations for operating electrical devices should be followed.
- 2) **AC MAINS CONNECTION:** While working with the npi systems, always adhere to the appropriate safety measures for handling electronic devices. Before using any device please read manuals and instructions carefully.  
The device is to be operated only at 115/230 Volt 60/50 Hz AC. Please check for appropriate line voltage before connecting any system to mains.  
Always use a three-wire line cord and a mains power-plug with a protection contact connected to ground (protective earth).  
Before opening the cabinet, unplug the instrument.  
Unplug the instrument when replacing the fuse or changing line voltage. Replace fuse only with an appropriate specified type.
- 3) **STATIC ELECTRICITY:** Electronic equipment is sensitive to static discharges. Some devices such as sensor inputs are equipped with very sensitive FET amplifiers, which can be damaged by electrostatic charge and must therefore be handled with care. Electrostatic discharge can be avoided by touching a grounded metal surface when changing or adjusting sensors. **Always turn power off when adding or removing modules, connecting or disconnecting sensors, headstages or other components from the instrument or 19" cabinet.**
- 4) **TEMPERATURE DRIFT / WARM-UP TIME:** All analog electronic systems are sensitive to temperature changes. Therefore, all electronic instruments containing analog circuits should be used only in a warmed-up condition (i.e. after internal temperature has reached steady-state values). In most cases a warm-up period of 20-30 minutes is sufficient.
- 5) **HANDLING:** Please protect the device from moisture, heat, radiation and corrosive chemicals.

## 2. EPMS-07 Modular Plug-In System

### 2.1. *General System Description / Operation*

The npI EPMS-07 is a modular system for processing of bioelectrical signals in electrophysiology. The system is housed in a 19" rackmount cabinet (3U) has room for up to 7 plug-in units. The plug-in units are connected to power by a bus at the rear panel.

The plug-in units must be kept in position by four screws (M 2,5 x 10). The screws are important not only for mechanical stability but also for proper electrical connection to the system housing. Free area must be protected with covers.

### 2.2. *EPMS-07 Housing*

The following items are shipped with the EPMS-07 housing:

- ✓ EPMS-07 cabinet with built-in power supply
- ✓ Mains cord
- ✓ Fuse 2 A / 1 A, slow
- ✓ Front covers

In order to avoid induction of electromagnetic noise the power supply unit, the power switch and the fuse are located at the rear of the housing.

### 2.3. *EPMS-E-07 Housing*

The following items are shipped with the EPMS-E-07 housing:

- ✓ EPMS-E-07 cabinet
- ✓ External Power supply PWR-03D
- ✓ Power cord (PWR-03D to EPMS-E-07)
- ✓ Mains chord
- ✓ Fuse 1.6 A / 0.8 A, slow
- ✓ Front covers

The EPMS-E-07 housing is designed for low-noise operation, especially for extracellular and multi channel amplifiers with plugged in filters. It operates with an external power supply to minimize distortions of the signals caused by the power supply.

### 2.4. *PWR-03D*

The external power supply PWR-03D is capable of driving up to 3 EPMS-E housings. Each housing is connected by a 6-pole cable from the one of the three connectors on the front panel of the PWR-03D to the rear panel of the respective EPMS-E housing. (see Figure 1, Figure 3). A POWER LED indicates that the PWR-03D is powered on (see Figure 1). Power switch, voltage selector and fuse are located at the rear panel (see Figure 2).

**Note:** The chassis of the PWR-03D is connected to protective earth, and it provides protective earth to the EPMS-E housing if connected.



Figure 1: PWR-03D front panel view



Figure 2: PWR-03D rear panel view

**Note:** This power supply is intended to be used with npi EPMS-E systems only.

## 2.5. System Grounding

### EPMS-07

The 19" cabinet is grounded by the power cable through the ground pin of the mains connector (= protective earth). In order to avoid ground loops the internal ground is isolated from the protective earth. The internal ground is used on the BNC connectors or GROUND plugs of the modules that are inserted into the EPMS-07 housing. The internal ground and mains ground (= protective earth) can be connected by a wire using the ground plugs on the rear panel of the instrument. It is not possible to predict whether measurements will be less or more noisy with the internal ground and mains ground connected. We recommend that you try both arrangements to determine the best configuration.



### EPMS-E-07

The 19" cabinet is connected to the CHASSIS connector at the rear panel. The CHASSIS is linked to protective earth as soon as the PWR-03D is connected. It can be connected also to the SYSTEM GROUND (SIGNAL GROUND) on the rear panel of the instrument (see Figure 3).

**Important:** Always adhere to the appropriate safety measures.

Figure 3: Rear panel connectors of the EPMS-E-07

## 2.6. Technical Data

19" rackmount cabinet, for up to 7 plug-in units

Dimensions: 3U high (1U=1 3/4" = 44.45 mm), 254 mm deep

### EPMS-07

Power supply: 115/230 V AC, 60/50 Hz, fuse 2 A / 1 A slow, 45-60 W

### EPMS-E-07

External power supply (for EPMS-E): 115/230 V AC, 60/50 Hz, fuse 1.6/0.8 A, slow

Dimensions of external power supply: (W x D x H) 225 mm x 210 mm x 85 mm

### 3. Introduction

npi electronic's SEC (Single Electrode Clamp) systems are based on the newest developments in the field of modern electronics and control theory (see also chapter 11). These versatile current/voltage clamp amplifiers permit extremely rapid switching between current injection and current-free recording of true intracellular potentials.

The use of modern high-voltage operational amplifiers and a new, improved method of capacity compensation makes it possible to inject very short current pulses through high resistance microelectrodes (up to 200 M $\Omega$  and more) and to record membrane potentials accurately, i.e. without series resistance error, within the same cycle.

Although the system has been designed primarily to overcome the limitations related to the use of high resistance microelectrodes in intracellular recordings, it can also be used to do conventional whole-cell patch clamp recordings with suction electrodes or perforated patch recordings. The whole-cell configuration allows to investigate even small dissociated or cultured cells as well as cells in slice preparations in both current and voltage clamp mode, while the intracellular medium is being controlled by the pipette solution.

#### 3.1. *Why a Single Electrode Clamp?*

Voltage clamp techniques permit the analysis of ionic currents flowing through biological membranes at preset membrane potentials. Under ideal conditions the recorded current is directly related to the conductance changes in the membrane and thus gives an accurate measure of the activity of ion channels and electrogenic pumps.

The membrane potential is generally kept at a preselected value (command or holding potential). Ionic currents are then activated by sudden changes in potential (e.g. voltage-gated ion channels), by transmitter release at synapses (e.g. electrical stimulation of fiber tracts in brain slices) or by external application of an appropriate agonist. Sudden command potential changes used to activate voltage-gated currents are especially challenging, because the membrane will adopt the new potential value only after it's capacitance ( $C_m$  in Figure 4 and Figure 5) has been charged. Therefore, the initial transient current following the voltage step should be as large as possible to achieve rapid membrane charging. In conventional patch clamp amplifiers, this requires a minimal resistance between the amplifier and the cell interior – a simple consequence of Ohm's law ( $\Delta U = R \cdot I$ ), i.e. for a given voltage difference ( $\Delta U$ ), the current ( $I$ ) is inversely proportional to the resistance ( $R$ ). In this context,  $R$  is the access or series resistance ( $R_a$  in Figure 4 and Figure 5) between the electrode and the cell interior. The time constant for charging a cell is  $\tau = R_{EL} \cdot C_m$ .

$R_a$  is largely determined by certain electrode properties (mainly electrode resistance) and the connection between the electrode and the cell. Typical  $R_a$  values are between 5 to 10 M $\Omega$ , which results in a time constant of 0.5 to 1 ms for a cell with a membrane capacity of 100 pF, i.e. the membrane needs roughly a millisecond to follow the command voltage step. Sharp microelectrodes usually have much larger resistances (30 to 150 M $\Omega$  or even more).

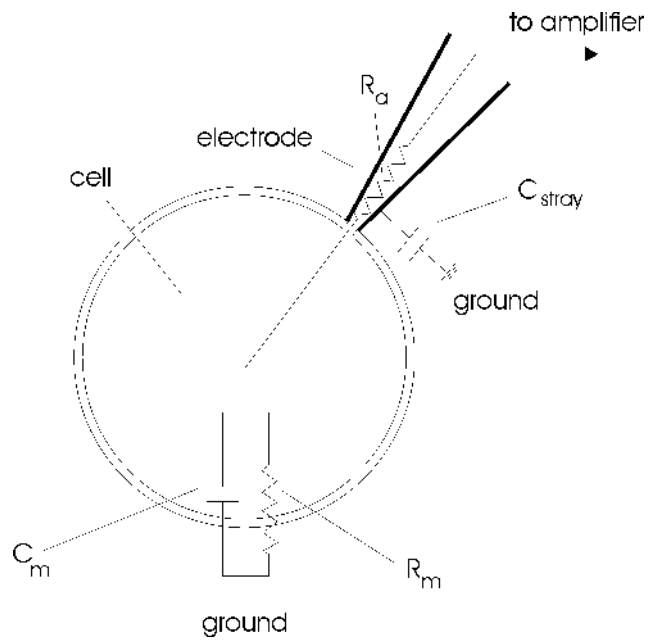


Figure 4: Model circuit for whole cell patch clamp recording using a suction electrode  
 $C_m$ : membrane capacitance,  $C_{stray}$ : electrode stray capacitance,  $R_{EL}$ : electrode resistance,  $R_m$ : membrane resistance

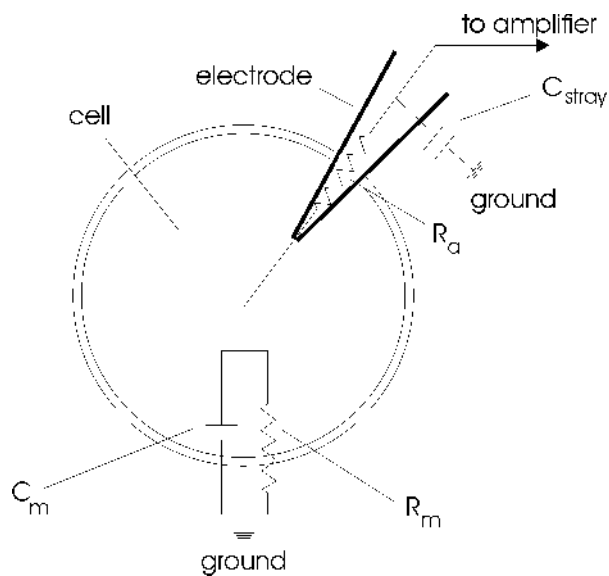


Figure 5: Model circuit for intracellular recording using a sharp electrode  
 $C_m$ : membrane capacitance,  $C_{stray}$ : electrode stray capacitance,  $R_{EL}$ : electrode resistance,  $R_m$ : membrane resistance

Besides slowing the voltage response of the cell,  $R_a$  can also cause additional adverse effects, such as error in potential measurement.  $R_a$ , together with the membrane resistance ( $R_m$ ) forms a voltage divider (see Figure 4 and Figure 5). Current flowing from the amplifier to the grounded bath of a cell preparation will cause a voltage drop at both,  $R_a$  and  $R_m$ . If  $R_a \ll R_m$ , the majority of the voltage drop will develop at  $R_m$  and thus reflect a true membrane potential. If, in an extreme case,  $R_a = R_m$ , the membrane potential will follow only one half of the voltage command. In order to achieve a voltage error of less than 1%  $R_a$  must be more than 100 times smaller than  $R_m$ . This condition is not always easily to accomplish, especially if recordings are performed from small cells. If sharp intracellular microelectrodes are used, it is virtually impossible. If  $R_a$  is not negligible, precise determination of the membrane potential can be achieved only if no current flows across  $R_a$  during potential measurement. This is the strategy employed in npi electronic's SEC amplifier systems.

The SEC amplifiers inject current and record the potential in an alternating mode (switched mode). Therefore, this technique is called discontinuous SEVC. This ensures that no current passes through  $R_a$  during potential measurement and completely eliminates access resistance artefacts.

After each injection of current, the potential gradient at the electrode tip decays much faster than the potential added at the cell membrane during the same injection. The membrane potential is measured after the potential difference across  $R_a$  has completely dropped (see chapter 3.2). The discontinuous current and voltage signal are then smoothed and read at the CURRENT OUTPUT and POTENTIAL OUTPUT connectors.

### 3.2. Principle of Operation

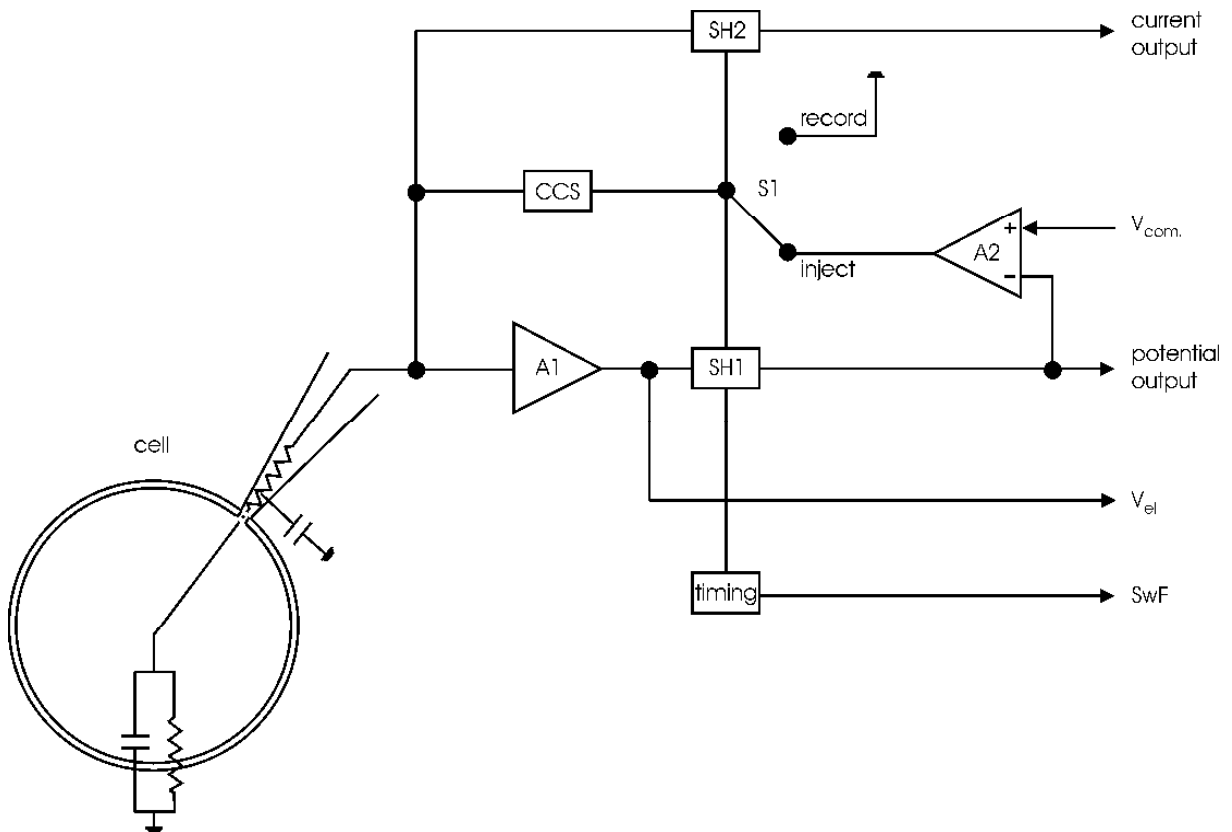


Figure 6: Model circuit of SEC systems

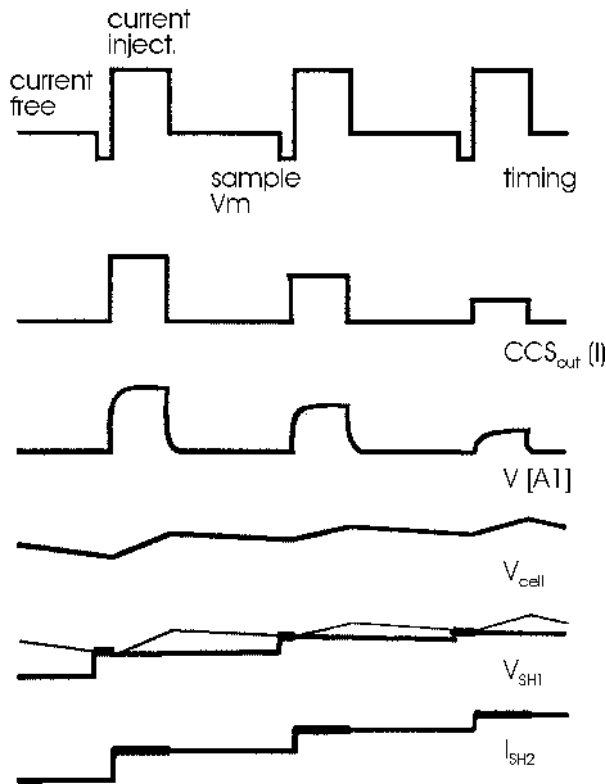


Figure 7: principle of SEVC operation

Figure 6 and Figure 7 illustrate the basic circuitry and operation of npI SEC voltage clamp amplifiers.

A single microelectrode penetrates the cell or is connected to the cell interior in the whole-cell configuration of the patch clamp technique. The recorded voltage is buffered by a  $\times 1$  operational amplifier (A1 in Figure 6). At this point, the potential ( $V[A1]$  in Figure 7) is the sum of the cell's membrane potential and the voltage gradient which develops when current is injected at the access resistance. Due to npI's unique compensation circuitry, the voltage at the tip of the electrode decays extremely fast after each injection of current and therefore allows for a correct measurement of  $V_m$  after a few microseconds. At the end of the current-free interval, when the electrode potential has dropped to zero, the sample-and-hold circuit (SH1 in Figure 6) samples  $V_m$  and holds the value for the remainder of the cycle ( $V_{SH1}$  in Figure 7).

The differential amplifier (A2 in Figure 6) compares the sampled potential with the command potential ( $V_{com}$  in Figure 6). The output of this amplifier becomes the input of a controlled current source (CCS in Figure 6), if the switch S1 (Figure 6) is in the current-passing position. The gain of this current source increases as much as  $100 \mu A/V$  due to a PI (proportional-integral) controller and improved electrode capacity compensation. In Figure 6 S1 is shown in the current-passing position, when a square current is applied to the electrode. When the current passes the electrode a steep voltage gradient develops at the electrode resistance.  $V_{cell}$  (Figure 7) is only slightly changed due to the slow charging of the membrane capacitance. The amplitude of injected current is sampled in the sample-and-hold amplifier SH2 (Figure 6), multiplied by the fractional time of current injection within each duty cycle (1/8 to 1/2 in SEC-05 and SEC-10, 1/4 in SEC-03 systems) and read out as current output ( $I_{SH2}$  in Figure 7). S1 then switches to the voltage-recording position (input to CCS is zero). The potential at A1 decays rapidly due to the fast relaxation at the (compensated) electrode capacity. Exact capacity compensation is essential to yield an optimally flat voltage trace at the end of the

current free interval when  $V_{\text{cell}}$  is measured (see also Figure 17). The cellular membrane potential, however, will drop much slower due to the large (uncompensated) membrane capacitance. The interval between two current injections must be long enough to allow for complete ( $\leq 1\%$ ) settling of the electrode potential, but short enough to minimize loss of charges at the cell membrane level, i.e. minimal relaxation of  $V_{\text{cell}}$ . At the end of the current-free period a new  $V_m$  sample is taken and a new cycle begins.

Thus, both current and potential output are based on discontinuous signals that are stored during each cycle in the sample-and-hold amplifiers SH1 and SH2. The signals will be optimal smooth at maximal switching frequencies.

#### *Major Advantages of the npi SEC System*

npi electronic's SEC amplifiers are the only systems that use a PI controller to avoid artificial recordings known to occur in other single electrode clamp systems ("clamping of the electrode"). The PI controller design increases gain to as much as  $100 \mu\text{A}/\text{V}$  in frequencies less than one-fourth the switching frequency. The result is very sensitive control of the membrane potential with a steady-state error of less than 1% and a fast response of the clamp to command steps or conductance changes.

The use of discontinuous current and voltage clamp in combination with high switching frequencies yields five major advantages:

1. The large recording bandwidth allows recordings of even fast signals accurately.
2. High clamp gains (up to  $100 \mu\text{A}/\text{V}$ ) can be used in voltage clamp mode.
3. Very small cells with relatively short membrane time constants can be voltage-clamped.
4. Series resistance effects are completely eliminated for a correct membrane potential control even with high resistance microelectrodes.
5. The true membrane potential is recorded also in the voltage clamp mode (whereas continuous feedback VC amplifiers only reflect the command potential).

### **3.3. Advantages of the Modular SEC-03M System**

The SEC-03M system is based on the well proven npi SEC technology and designed as a module for the EPMS-07 system. Several combinations with other modules are possible.

Because this amplifier is small and handy, it is possible to combine up to three synchronized SEC-03M in one 19" EPMS-07 housing, e.g. for recording from coupled cells simultaneously. For recording from one cell only, it is recommended to add one or two filters to the SEC-03M module. Such a recording system can further be enhanced by adding a stimulus isolator, a iontophoretic amplifier or a controller for pressure ejection.

When using CellWorks the combination with the modular breakout box INT-20M facilitates building-up a setup. All signals from or to amplifiers or filters in an EPMS housing can be linked to each other, and directly to the breakout box making additional BNC cabling unnecessary.

Two additional modules (HVC-03M and PEN-03) can supplement an SEC-03M amplifier in order to allow one and two electrode voltage clamp experiments with enhanced cell penetration facilities.

Please ask npi for an optimal configuration according to your needs.

## 4. SEC-03M System

### 4.1. SEC-03M Components

The following items are shipped with the SEC-03M system:

- ✓ Amplifier module for the EPMS-07 system
- ✓ Headstage
- ✓ GND- and DRIVEN SHIELD (2.6 mm banana plug) connectors

Please open the box and inspect contents upon receipt. If any components appear damaged or missing, please contact npielectronic or your local distributor immediately (support@npielectronic.com).

Optional accessories:

- ⇨ Electrode holder set with one holder for sharp microelectrodes (without port), one suction (patch) electrode holder (with one port) and an electrode holder adapter (SEC-EH-SET)



- ⇨ Active cell model (SEC-MODA)
- ⇨ Passive cell model (SEC-MOD, see chapter 7)
- ⇨ Low noise / low bias current headstage (SEC-HSP) with a reduced current range (:10 headstage, i.e. maximal current is  $\pm 12$  nA)
- ⇨ Headstage with differential input (SEC-HSD)
- ⇨ Headstage for extracellular measurements (SEC-EXT)
- ⇨ Filter for the EPMS system
- ⇨ Data acquisition module
- ⇨ Stimulus isolator module
- ⇨ Iontophoresis module
- ⇨ Pressure ejection module
- ⇨ CellWorks hard- and software

## 4.2. Description of the Front Panel

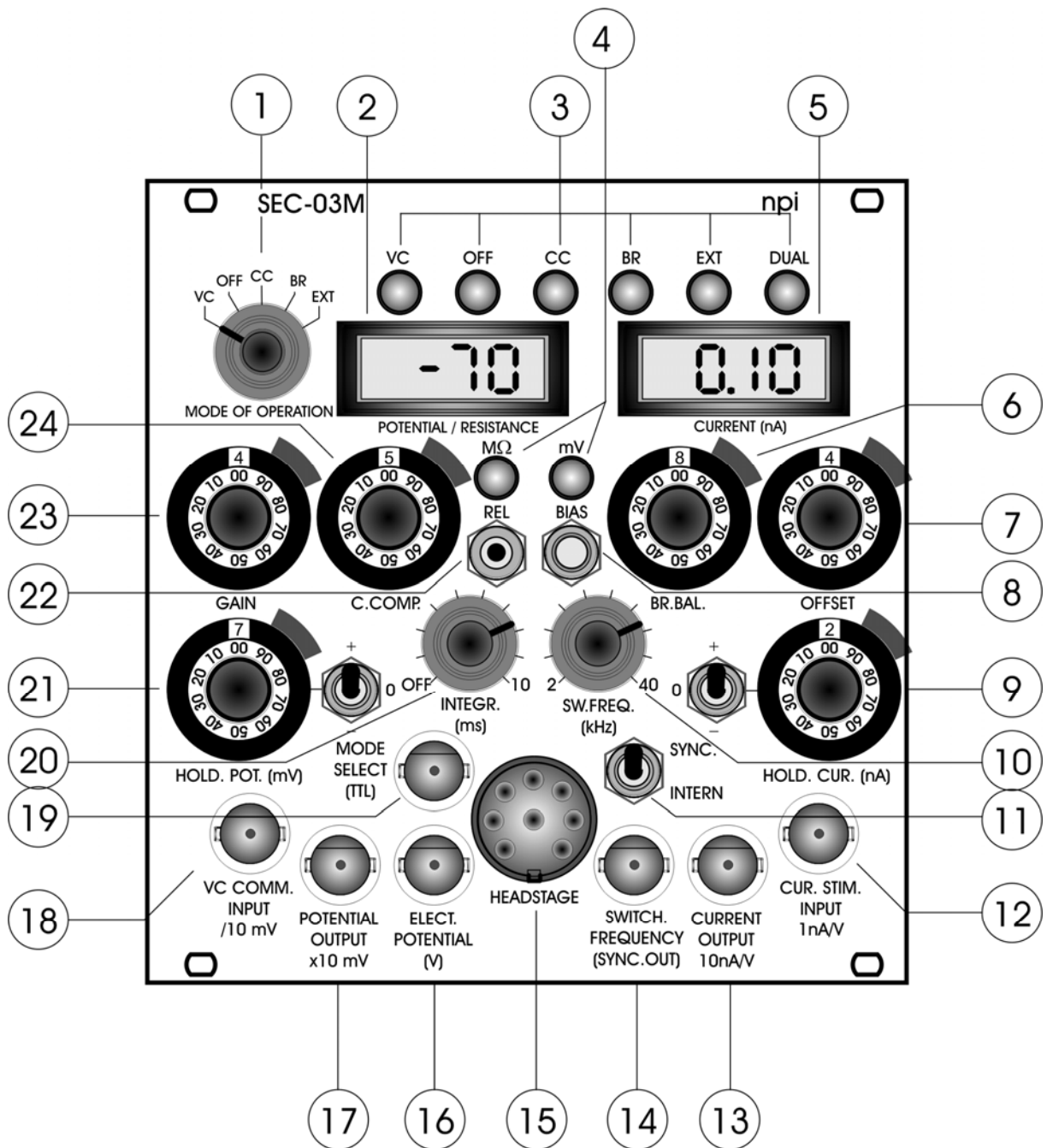


Figure 8: SEC-03M front panel view

In the following description of the front panel elements each element has a number that is related to that in Figure 8. The number is followed by the name (in uppercase letters) written on the front panel and the type of the element (in lowercase letters). Then, a short description of the element is given. Each control element has a label and frequently a calibration (e.g. CURRENT OUTPUT, 10nA/V).

(1) MODE OF OPERATION switch



VC: Voltage Clamp

OFF: voltage- and current clamp OFF. In this position the amplifier does not apply any voltage or current to the cell. The potential at the electrode tip is measured and displayed. The BUZZ function is active.

CC: Current Clamp

BR: Bridge Mode

EXT.: EXTERNAL control; if this position is selected, the mode of operation (VC, CC) can be set by a TTL pulse applied to the MODE SELECT BNC (19); TTL high = VC; TTL low = CC.

(2) POTENTIAL / RESISTANCE display



LC-Display for the POTENTIAL at the electrode tip in mV or the electrode RESISTANCE in  $M\Omega$ .

(3) MODE OF OPERATION LEDs (VC, OFF, CC, BR, EXT, DUAL)



LEDs indicating the active mode of operation (see also #1). If operated together with the HVC-03M module the DUAL LED indicates that the SEC-03M works in two electrode voltage clamp mode.

(4)  $M\Omega$  / mV LEDs



LEDs indicating that RESISTANCE ( $M\Omega$ ) or POTENTIAL (mV) is revealed in DISPLAY (#2).

(5) CURRENT display



LC-Display for the CURRENT passed through the CURRENT electrode in nA (X.XX nA).

(6) BR.BAL. potentiometer



If current is passed through the recording electrode the potential deflection caused at the electrode resistance is compensated with this control (ten turn potentiometer, clockwise, calibrated in  $M\Omega$ , range: 0-1000  $M\Omega$ ).

(7) OFFSET potentiometer



Control to set the output of the electrode preamplifier to zero (ten-turn potentiometer, symmetrical, i.e. 0 mV = 5 on the dial), range:  $\pm 200$  mV.

**Note:** Position 5 on the OFFSET control corresponds to 0 mV offset.

(8) BIAS (bias current) potentiometer



With this trim potentiometer the output current of the headstage (headstage BIAS current) can be tuned to zero

(9) HOLD.CUR.(nA) potentiometer and polarity switch



10-turn digital control that presets a continuous command signal for CC mode (HOLD current). Polarity is set by switch to the left of the control (0 is off-position).

(10) SW.FREQ. (kHz) potentiometer



Potentiometer for setting the switching frequency in VC or CC mode; range 2 kHz to 40 kHz.

(11) SYNC. / INTERN switch

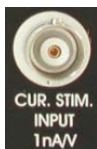


Switch for setting the synchronization mode of the switching frequency.

SYNC.: Switching frequency is synchronized with the “Master” amplifier for double cell recordings. SW.FREQ. potentiometer (#10) is disabled and the switching frequency is set by the “Master” amplifier.

INTERN: Switching frequency is set by SW.FREQ. potentiometer (#10) for single cell recordings.

(12) CUR.STIM. INPUT 1 nA/V connector



Analog input BNC connector for application of signals from an external stimulus source. The voltage signal that is connected here is transformed to a proportional current at the electrode with a sensitivity of 1 nA/V, i.e. an input voltage of 5 V is transformed to an output current of 5 nA. The signal form remains unchanged. The amplitude of the output current signal (current stimulus) is determined by the amplitude of the CUR.STIM. INPUT. Two examples are given in Figure 9. In **A** the amplitude of the CUR.STIM. INPUT is 1 V that gives a current stimulus of 1 nA, in **B** the CUR.STIM. INPUT amplitude is 2 V that is transformed into a current stimulus of 2 nA.

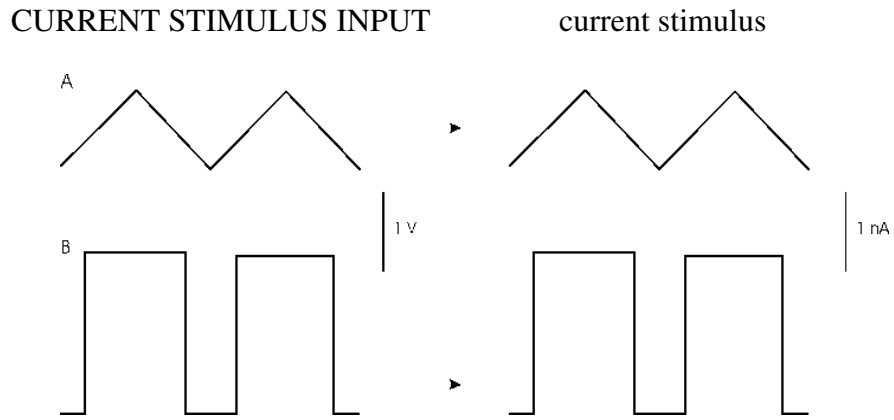


Figure 9: Input-output relation using CUR.STIM. INPUT

**Important:** The current injected through the electrode is always the sum of the input signal at CUR.STIM. INPUT (12) and the holding current set by HOLD.CUR. (9) and polarity switch.

(13) CURRENT OUTPUT 10 nA/V connector



BNC connector providing the CURRENT OUTPUT signal; scaling 10 nA / V, i.e. 1V corresponds to 10 nA.

(14) SWITCH. FREQUENCY (SYNC.OUT) connector



BNC connector providing the switching frequency for synchronization of an oscilloscope (triggering) for tuning the capacity compensation.

(15) HEADSTAGE connector



The HEADSTAGE cable is connected to the unit at this 12-pin connector in the center of the module.

(16) ELECT. POTENTIAL connector



BNC connector providing the switched signal directly from the electrode. This signal is used for tuning the capacity compensation (see also SEC-05 manual).

**(17) POTENTIAL OUTPUT x10 mV connector**

BNC connector monitoring the recorded membrane potential with a gain of ten.

**(18) VC COMM. INPUT /10 mV connector**

BNC connector for an external COMMAND in VC mode (sensitivity: /10, i.e. 0.1 V / V).

The voltage signal that is connected here is transformed to a proportional COMMAND voltage in VC mode. The signal form remains unchanged. Two examples are given in Figure 9. The amplitude of the output voltage signal (voltage stimulus) is determined by the amplitude of the input voltage signal.

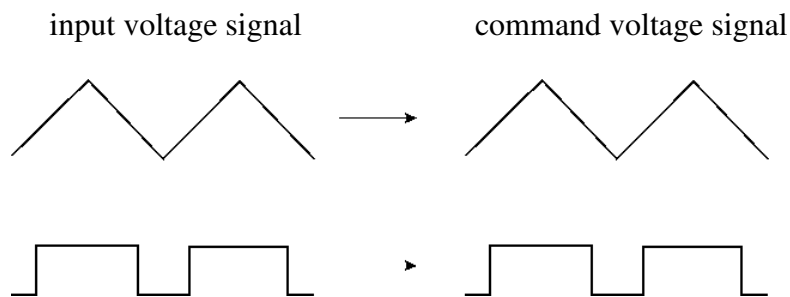


Figure 10: input-output relation using VC COMM. INPUT in VC mode

**(19) MODE SELECT connector**

BNC connector for remote control of the MODE of operation. A TTL signal is connected here to select the mode of operation remotely (HI = VC, LO = CC).

**(20) INTEGR. (ms) potentiometer**

Potentiometer for setting the INTEGRATOR time constant in VC mode; range: 0 to 10 ms.

**(21) HOLD. POT. (mV) potentiometer**

10-turn digital control that presets a continuous command signal (HOLD potential) for VC. Polarity is set by switch to the right of the control (0 is off-position).

**(22)** REL push button

Push button for activating the resistance measurement of the microelectrode. When pushed the microelectrode resistance is measured and shown in POTENTIAL / RESISTANCE display (#2).

***Important:*** An accurate measurement of  $R_{EL}$  requires that the input capacity is well compensated (see also #24 and chapter 8.6)

**(23)** GAIN potentiometer

10-turn potentiometer to set amplification factor (GAIN) of the VC error signal. To keep the VC error as small as possible it is necessary to use high GAIN settings, but the system becomes unstable and begins to oscillate if the GAIN is set too high. Thus, the care should be taken when setting this control. Using the INTEGRATOR (#20) provides a virtually infinite GAIN for slow signal, e.g. holding potential.

**(24)** C. COMP. potentiometer

Control for the capacity compensation of the microelectrode (ten turn potentiometer, clockwise).

***Caution:*** This circuit is based on a positive feedback circuit. Overcompensation leads to oscillations that may damage the cell.

## 5. Headstages

### 5.1. *Standard and low-noise (SEC-HSP) headstages*

The SEC-03M comes with the standard headstage (range:  $\pm 120$  nA) for connecting glass electrodes with high resistances or suction electrodes for whole cell patch clamp recordings with lower resistances via an electrode holder.

A low noise current headstage for measurement of small currents, a headstage with differential input and a headstage for extracellular measurements is also available (see chapter 5.2)

The electrode filled with electrolyte is inserted into an electrode holder (optional, see Figure 11) that fits into the electrode holder adapter (optional, see also **Optional accessories** in chapter 4.1). The electrical connection between the electrolyte and the headstage is established using a carefully chlorinated silver wire. Chlorinating of the silver wire is very important since contact of silver to the electrolyte leads to electrochemical potentials causing varying offset potentials at the electrode, deterioration of the voltage measurement etc. (for details see Kettenmann and Grantyn (1992)). For optimal chlorinating of silver wires an automated chlorinating apparatus (ACL-01) is available (contact npi for details).

GROUND provides system ground and is linked to the bath via an agar-bridge or a Ag-AgCl pellet. The headstage is attached to the amplifier with the headstage cable (see #1, Figure 11) and a 12-pole connector. The headstage is mounted to a holding bar that fits to most micromanipulators.

**Note:** The shield of the SMC connector is linked to the driven shield output and must not be connected to ground. The headstage enclosure is grounded.

**Caution:** Please always adhere to the appropriate safety precautions (see chapter 0). Please turn power off when connecting or disconnecting the headstage from the HEADSTAGE connector!

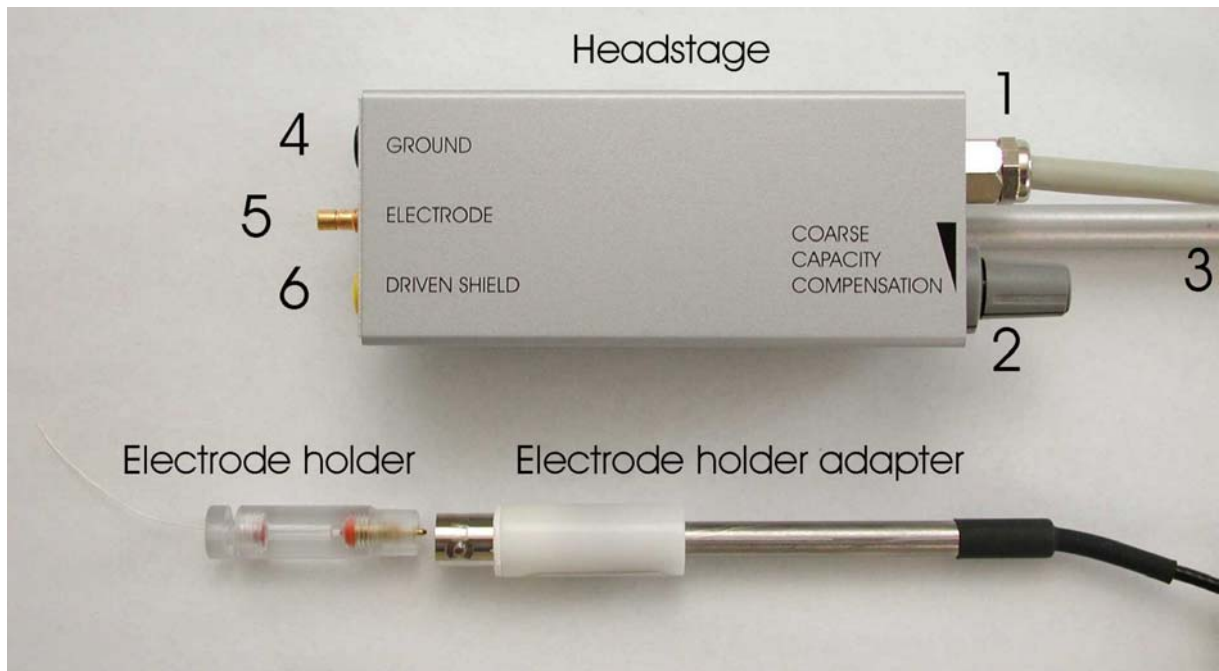


Figure 11: standard headstage, electrode holder (optional) and electrode holder adapter (optional) of the SEC-03M

The standard headstage consists of the following elements (see Figure 11):

- 1 Headstage cable to amplifier
- 2 Coarse capacity compensation potentiometer
- 3 Holding bar
- 4 GROUND: Ground connector
- 5 ELECTRODE: SMB connector for microelectrode
- 6 DRIVEN SHIELD connector

## 5.2. Low-noise headstage (SEC-HSP)

The low-noise / low bias headstage (range:  $\pm 12$  nA, see also **Optional accessories** in chapter 4.1) has an external capacity compensation and a BNC electrode holder connector.

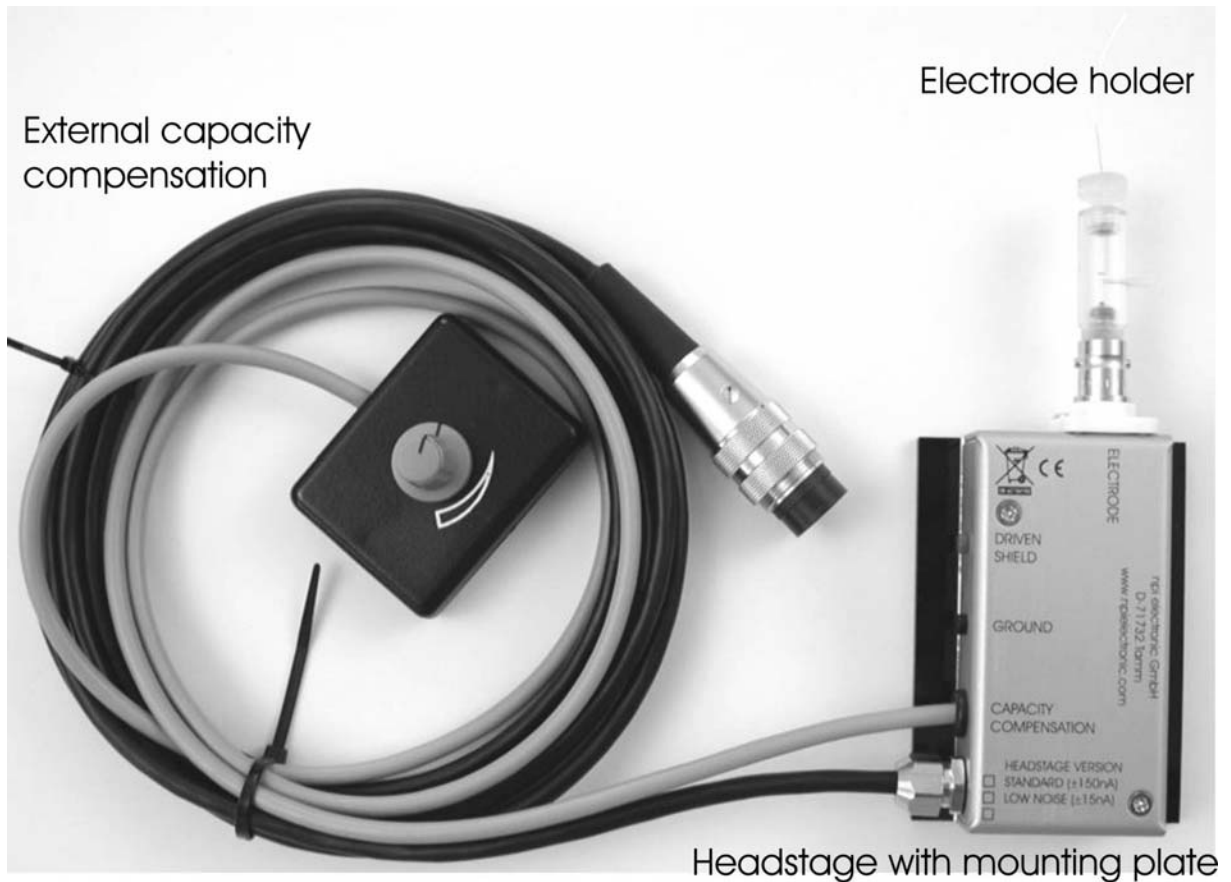


Figure 12: low noise headstage with electrode holder (optional)

The headstage is mounted to a non-conducting mounting plate.

**Note:** The shield of the BNC connector is linked to the driven shield output and must not be connected to ground. The headstage enclosure is grounded.

**Caution:** Please always adhere to the appropriate safety precautions (see chapter 1). Please turn power off when connecting or disconnecting the headstage from the HEADSTAGE connector!

## 6. Setting up the SEC-03M System

The following steps should help you set up the SEC-03M correctly. Always adhere to the appropriate safety measures (see chapter 1).

Usually the SEC-03M is shipped mounted in an EPMS-07 housing. If a single SEC-03M module is delivered, the user has to mount the module into the EPMS-07 housing. This is done by performing the basic installation steps.

### ① Basic installation

- Turn off the EPMS-07 system.
- Remove two front covers from the EPMS-07 housing.
- Plug in the SEC-03M and fasten the amplifier module with four screws. The screws are important not only for mechanical stability but also for proper electrical connection to the EPMS-07 housing.

After installation, the SEC-03M is attached to the setup by assembling the electrical connections. It is assumed that a cell model will be attached.

### ② Electrical connections

- Connect the headstage to the HEADSTAGE connector (#15, Figure 8) at the SEC-03M.
- Connect a cell model (see chapter 7) if you want to test the system with a cell model.
- Connect a digital/analog timing unit or a stimulation device to CUR. STIM. INPUT for CC experiments and / or to VC COMM. INPUT for VC experiments.
- Connect a store oscilloscope or a data recording device (i.e. a computer with data acquisition card) to the POTENTIAL OUTPUT and to the CURRENT OUTPUT, triggered from the stimulation device.

Before using the SEC-03M always start with the basic settings to avoid oscillations.

### ③ Basic settings

- Turn all controls to low values (less than 1) and the OFFSET in the range of 5 (zero position, see chapter 8.3).
- Set MODE OF OPERATION to BR (bridge mode).
- Turn POWER switch on.

Now the SEC-03M is ready for an initial check with the cell model.

***Important:*** All signal outputs are coarse and unfiltered directly from the headstages. Thus, we recommend to use always additional filters for signal conditioning.

## 7. Passive Cell Model

The SEC-03M can be ordered with a passive SEC (Single Electrode Clamp amplifier) cell model as an optional accessory. An active cell model is also available on request (for ref. see Draguhn et al. (1997)).

The cell model is designed to be used to check the function of the SEC amplifier either

1. to train personnel in using the instrument or
2. in case of trouble to check which part of the setup does not work correctly e.g. to find out whether the amplifier is broken or if something is wrong with the electrodes or holders etc.

The passive cell model consists only of passive elements, i.e. resistors that simulate the resistance of the cell membrane and the electrodes, and capacitances that simulate the capacitance of the cell membrane. A switch allows simulation of two different cell types: a “medium sized” cell with 100 M $\Omega$  membrane resistance and 100 pF membrane capacitance, or a “small” cell with 500 M $\Omega$  and 22 pF. Electrode immersed into the bath or SEAL formation can be mimicked as well. The headstage of the amplifier can be connected to one of two different types of electrodes (see below).

### 7.1. Cell Model Description

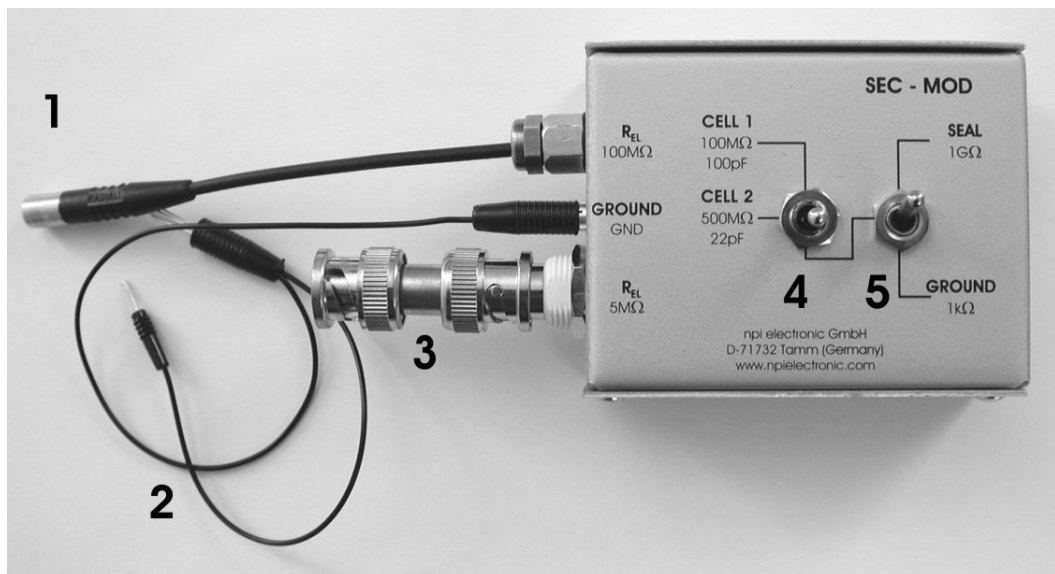


Figure 13: SEC-MOD passive cell model

- 1, 3: connectors for the headstage, 1: electrode resistance: 100 M $\Omega$ , 3: electrode resistance: 5 M $\Omega$
- 2: GND ground connector, to be connected to GND jack of the headstage
- 4: CELL: switch for cell membrane representing a membrane of either 100 M $\Omega$  and 100 pF (CELL 1) or 500 M $\Omega$  and 22 pF (CELL 2).
- 5: In GROUND (lower) position the electrodes are connected to ground via a 1 k $\Omega$  resistor. In SEAL (upper) position are connected to a 1 G $\Omega$  resistor simulating the formation of a GIGASEAL with a patch electrode.

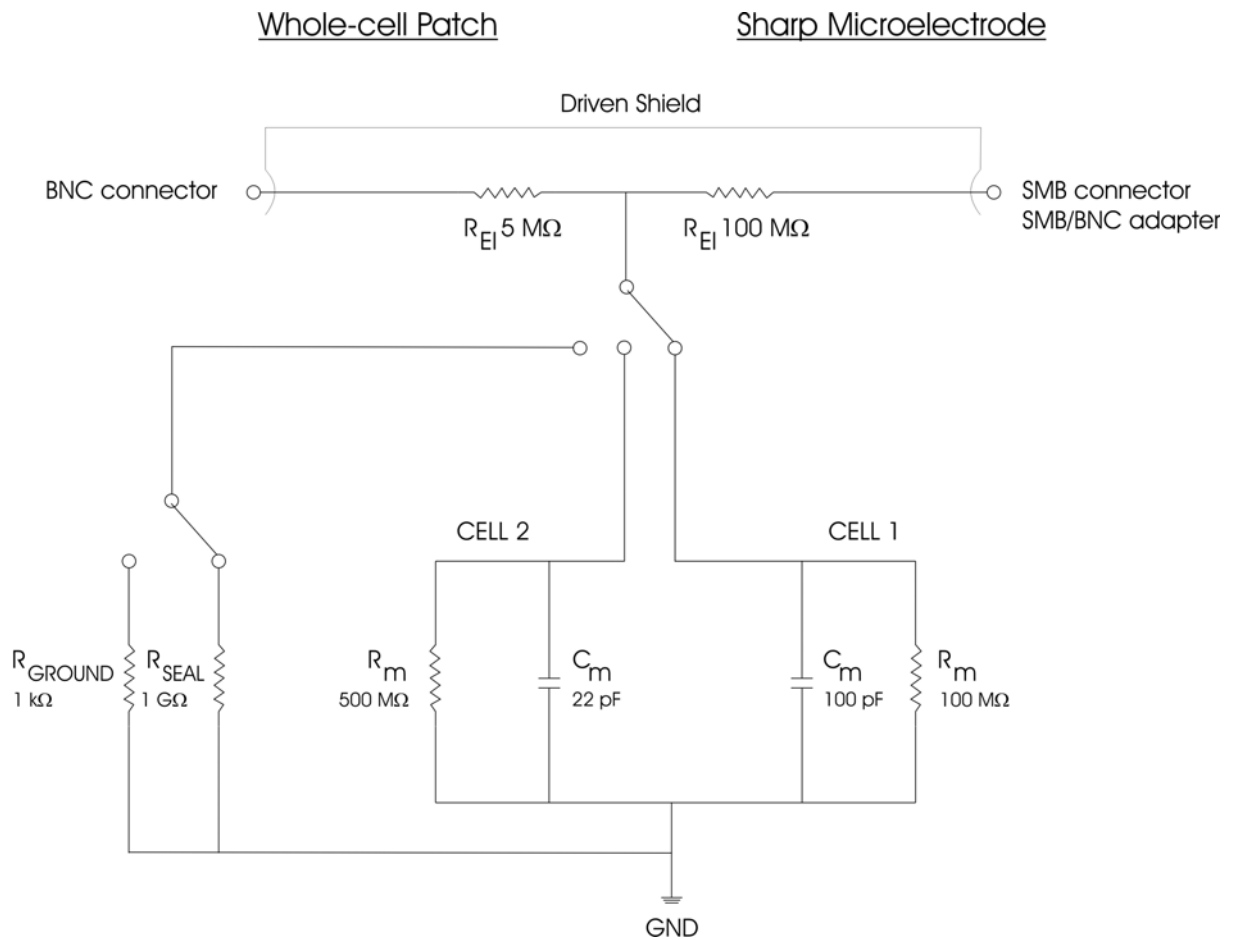


Figure 14: Schematic diagram of the passive cell model

## 7.2. Connections and Operation

### Connections

- Turn POWER switch of the amplifier off.
- a) For simulation of an experiment using a suction electrode
  - Connect the BNC jack of the cell model to the BNC connector P<sub>EL</sub> of the headstage.
- b) For simulation of an experiment using a sharp electrode
  - Connect the SMB connector of the cell model to the BNC connector P<sub>EL</sub> at the headstage. For headstages with BNC connector use the supplied SMB to BNC adapter.

For a) and b)

- Connect GND of the cell model to GND of the headstage.
- Do not connect DRIVEN SHIELD

### Simulation of electrode in the bath

- Set switch #4, Figure 13 to the lower position.
- Set switch #5, Figure 13 to GROUND position. The 1 k $\Omega$  resistor simulates the resistance of the bath solution. This can be used to train cancellation of offsets, using the bridge balance and using the capacity compensation.

### Simulation of SEAL formation

- Set switch #4, Figure 13 to the lower position.
- Set switch #5, Figure 13 to SEAL position. The 1 G $\Omega$  resistor simulates the SEAL resistance when forming a GIGASEAL in patch clamp experiments.

### Simulation of intracellular recording

Intracellular recordings can be mimicked with one of two cells with different properties. Use the 100 M $\Omega$  electrode connector (#1, Figure 13) for an experiment with sharp electrodes or the 5 M $\Omega$  electrode connector (#3, Figure 13) for simulating an experiment with patch electrodes.

- Switch the CELL membrane switch (see #4, Figure 13) to the desired position (CELL 1 or CELL 2).
- Turn all controls at the amplifier to low values (less than 1) and the OFFSET in the range of 5 (zero position) and the OSCILLATION SHUTOFF in the DISABLED position.
- Turn POWER switch of the amplifier on.

Now you can adjust the amplifier (see below) and apply test pulses to the cell model. The upper position the CELL membrane switch (CELL 1) simulates a cell with a resistance of 100 M $\Omega$  and a capacitance of 100 pF. In the lower position (CELL 2) a cell membrane with 500 M $\Omega$  and 22 pF is simulated.

## **7.3. Connections and Operation**

### Checking the configuration

- Turn POWER switch of the amplifier off.
  - a) For simulation of an experiment using a suction electrode
    - Connect the BNC jack of the cell model to the BNC connector P<sub>EL</sub> of the headstage.
  - b) For simulation of an experiment using a sharp electrode
    - Connect the SUBCLICK connector of the cell model to the BNC connector P<sub>EL</sub> at the headstage. For headstages with BNC connector use the supplied SMB to BNC adapter.

For a) and b)

- Connect GND of the cell model to GND of the headstage.

- Leave REF untouched.
- Switch the CELL membrane switch (see Figure 13) to the desired position.
- Turn all controls at the amplifier to low values (less than 1) and the OFFSET in the range of 5 and the OSCILLATION SHUTOFF in the DISABLED position.
- Turn POWER switch of the amplifier on.

Now you can adjust the amplifier (see below) and apply test pulses to the cell model. Connection to the BNC jack gives access to the cell via an electrode with 5 M $\Omega$  resistance. Connection to SUBCLICK adapter simulates access to the cell via an electrode with 100 M $\Omega$  resistance. The upper position the CELL membrane switch simulates a small cell with a resistance of 100 M $\Omega$  and a capacitance of 100 pF. In the lower position a cell membrane with 20 M $\Omega$  and 500 pF is simulated. The middle position simulates the electrode immersed into the bath and can be used to train cancellation of offsets, and using the capacity compensation.

## 8. Test and Tuning Procedures

**Important:** The SEC-03M should be used only in warmed-up condition i.e. 20 to 30 minutes after turning power on.

The following test and tuning procedures are necessary for optimal recordings. It is recommended to first connect a cell model to the amplifier to perform some basic adjustments and to get familiar with these procedures. It is assumed that all connections are built as described in chapter 6. Many of the tuning procedure can be performed analogue to those described in the manual for the SEC-05LX.

**Important:** Except for *Headstage bias current adjustment* (see 8.1) all adjustments described below should be carried out every time before starting an experiment or after changing the electrode.

### 8.1. Headstage Bias Current Adjustment

**Caution:** It is important that this tuning procedure is performed ONLY after a warm-up period of at least 30 minutes!

This tuning procedure is very important since it determines the accuracy of the SEC system. Therefore it must be done routinely with great care.

SEC systems are equipped with a current source that is connected to the current injecting electrode and performs the current injection. This current source has a high-impedance floating output. Therefore the zero position (the zero of the bias current i.e. with no input signal there is no output current) of this device has to be defined.

Since the highly sensitive FET amplifiers in the headstage become warm from the internal heat dissipation and their characteristics are strongly temperature dependent, the calibration procedure has to be done periodically by the user.

The tuning procedure is done in BR MODE using the BIAS control (#8, Figure 8, range approx.  $\pm 500$  pA) and a resistance of a few ten M $\Omega$  or a cell model. It is based on Ohm's Law: The voltage deflection caused by the bias current generated by the headstage on a test resistor is displayed on the digital meter. The output current that is proportional to the monitored voltage deflection is tuned to zero with the HEADSTAGE BIAS CURRENT control.

This tuning procedure cannot be performed with an electrode since there always are unknown offset voltages involved (tip potential, junction potentials etc.). Therefore a test resistor of 10-100 M $\Omega$  must be used. The procedure is described step by step.

- ❑ First, the headstage electrode connector must be grounded (as if an electrode with a very low resistance were attached). To avoid damage of the headstage amplifiers please use a 10 k $\Omega$  resistor (which is small enough compared to a 10-100 M $\Omega$  resistor). Now the offset potential of the POTENTIAL output can be tuned to zero. Watch the left digital display and set the POTENTIAL output to zero with the OFFSET control.
- ❑ Next, a resistance of 10-100 M $\Omega$  is connected from the headstage output to ground (as if an electrode with a high resistance were attached).
- ❑ The left digital display (and the POTENTIAL OUTPUT BNC connector (x10mV)) now show a voltage deflection which is proportional to the flowing output current (bias current).
- ❑ This bias current can be tuned to zero with the BIAS control. The current is zero when the voltage deflection is zero (i.e. the meter shows zero).
- ❑ As a rule, the current output (CURRENT OUTPUT BNC) and the CURRENT DISPLAY (lower digital display) should also read zero.

***Important:*** All headstages are equipped with very sensitive FET amplifiers, which can be damaged with electrostatic charge and must therefore be handled with care. This can be avoided by touching a grounded metal surface when changing or adjusting the electrodes. If a headstage is not used the input should always be connected to ground (either using an appropriate connector or with aluminum foil wrapped around the headstage). Always turn power off when connecting or disconnecting headstages from the 19" cabinet.

## **8.2. Electrode Selection**

Electrodes must be tested before use. This is done by applying positive and negative current pulses. Electrodes which show significant changes in resistance (rectification) cannot be used for intracellular recordings. By increasing the current amplitude the capability of the electrode to carry current can be estimated. The test current must cover the full range of currents used in the experiment. Sometimes the performance of electrodes can be improved by breaking the tip.

## **8.3. Offset Compensation**

If an electrode is immersed into the bath solution an offset voltage will appear, even if no current is passed. This offset potential is the sum of various effects at the tip of the electrode filled with electrolyte ("tip potential", junction potential etc.). This offset voltage must be compensated, i.e. set to zero carefully with the OFFSET control (#7, Figure 8) before recording from a cell. When adjusting the OFFSET make sure that no current flows through the electrode. Thus, it is recommended to disconnect all inputs.

If a cell model is connected the OFFSET control should read a value around 5, otherwise it is likely that the headstage or the amplifier is damaged.

#### 8.4. Bridge Balance (in BR mode)

If current is passed through an electrode the occurring voltage deflection (potential drop at  $R_{EL}$ ) affects the recording of membrane potential in BRIDGE mode. Therefore this deflection must be compensated carefully by means of the BR. BAL. control. This control is calibrated in  $M\Omega$ .

With the cell model connected or the electrode in the bath the BR. BAL. control is turned on clockwise until there is no artifact on the POTENTIAL OUTPUT (see Figure 16).

- Make the basic settings at the amplifier (see chapter 6).
- Connect a cell model or immerse the electrode into the bath as deep as necessary during the experiment.
- Apply current pulses to the electrode either using an external stimulator (via the CUR. STIM. INPUT connector (#12, Figure 8).
- Watch the POTENTIAL OUTPUT at the oscilloscope and adjust the BRIDGE BALANCE as shown in Figure 16 using the BR. BAL. potentiometer (#6, Figure 8). After adjustment you should see a straight voltage trace without artifacts caused by the potential drop at  $R_{EL}$ .

Figure 16 illustrates the BRIDGE BALANCE procedure using a  $100 M\Omega$  resistor that represents the electrode. The current stimulus amplitude was set to  $0.5 nA$ . In the upper diagram the bridge is slightly undercompensated and in the diagram in the middle it is slightly overcompensated. The lower diagram shows a well balanced bridge (compensated).

**Important:** BRIDGE BALANCE must be tuned several times during an experiment since most parameters change during a recording session (see Figure 15)

OFFSET deviations can be detected by comparing the readout on the potential display before and after an experiment (with the electrode in the tissue, but not in a cell).

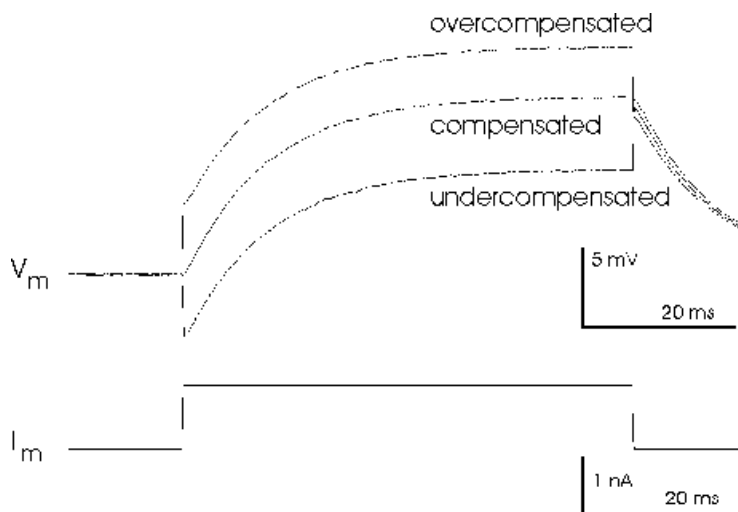


Figure 15: Adjustment of the bridge balance after cell penetration (in BR mode)

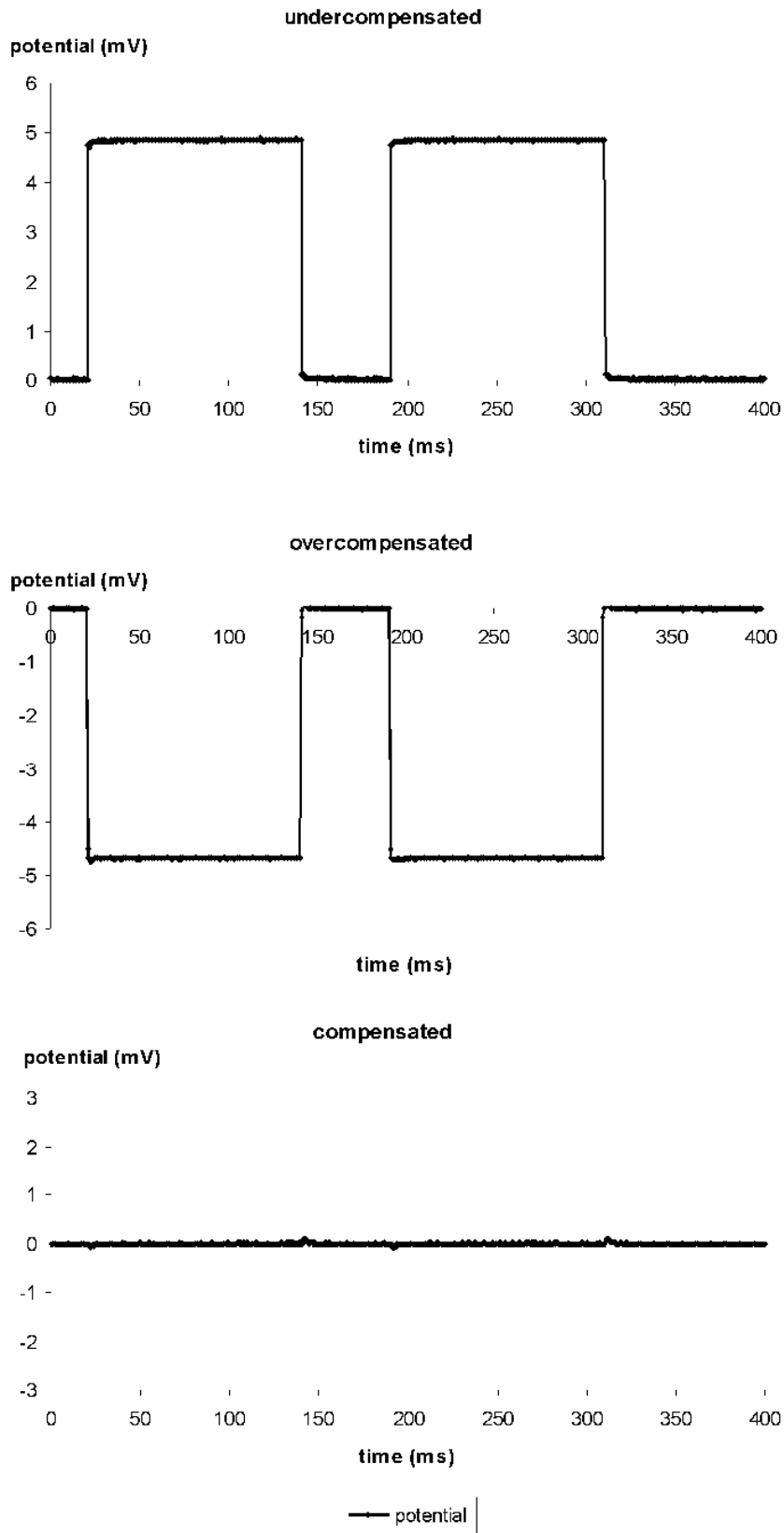


Figure 16: Tuning of the BRIDGE BALANCE using 100 MΩ resistor

## 8.5. **Switching Frequency and Capacitance Compensation (in switched modes)**

For accurate measurements in switched mode, it is **essential** that the capacity of the electrode is fully compensated.

***Important:*** Wrong compensation of electrode capacity leads to errors in measurements done in switched mode of the amplifier (see Figure 18).

***Microelectrode selection:*** As depicted in chapter 8.2 electrodes must be tested before use. For details see also Richter et al., 1996.

Switching frequency is a key parameter of discontinuous single electrode clamp (dSEVC) systems. The switching frequency determines the accuracy, speed of response, and signal-to-noise ratio of the dSEVC system (Richter et al., 1996; Muller et al., 1999). Since its launch in 1984, one of the outstanding features of the SEC series of single electrode voltage / current clamp systems has been the ability to record routinely with high switching frequencies in the range of tens of kilohertz, regardless of the microelectrode resistance (Polder et al., 1984). Principles of the dSEVC technique are described in chapter 3.2 and in (Polder et al., 1984; Polder & Swandulla, 2001).

*Looking back:* In the early eighties, when the design of the SEC 1L system was started, single electrode clamping began to gain importance beside the two classical intracellular methods: bridge recording or whole cell patch clamp recording. The great advantage compared to the whole cell recording method using a patch amplifier was the elimination of series resistance due to the time sharing protocol (see also chapter 3.2). No current flow during voltage recording means no interference from the series resistance regardless of its value. Thus, voltage clamp recordings with sharp microelectrodes in deep cell layers became possible. The historical weak point of this method was the low switching frequency due to the fact that stray capacities around the microelectrode could not be compensated sufficiently.

The SEC systems provides a solution for this problem. With their improvements on capacity compensation electronics, they can be used with switching frequencies of tens of kHz even with high resistance microelectrodes. What are the technical principles that make possible such high switching frequencies?

In SEC systems a special protocol is used to rapidly compensate the microelectrode. Figure 17 shows the compensation scheme of a sharp microelectrode immersed 3 mm into the cerebrospinal fluid. Here the increase in speed can be seen clearly. Recordings under such conditions and possible applications have been presented in several papers (e.g. Richter et al., 1996).

### *Criteria for the selection of the switching frequency*

Which are the most important criteria for the selection of the switching frequency? This question was analyzed in detail by M. Weckstrom and colleagues (Juusola 1994; Weckstrom et al., 1992). They presented a formula that describes the conditions for obtaining reliable results during a switching single electrode clamp:

$$f_e > 3f_{sw}, f_{sw} > 2f_s, f_s > 2f_f > f_m$$

- $f_e$ : upper cutoff frequency of the microelectrode  
 $f_{sw}$ : switching frequency of the dSEVC  
 $f_s$ : sampling frequency of the data acquisition system  
 $f_f$ : upper cutoff frequency of the lowpass filter for current recording,  
 $f_m$ : upper cutoff frequency of the membrane.

**Example** (Muller et al., 1999): With the time constant of 1-3  $\mu$ s recorded for the electrodes used in this study,  $f_e$  is 80-160 kHz, the selected switching frequency of the dSEVC was 30 – 50 kHz (calculated range is 25-53 kHz), data were sampled at 10 kHz and the current signals have been filtered at 5 kHz. These settings are currently used for recordings in many labs.

The principle of operation in switched mode is shown below.

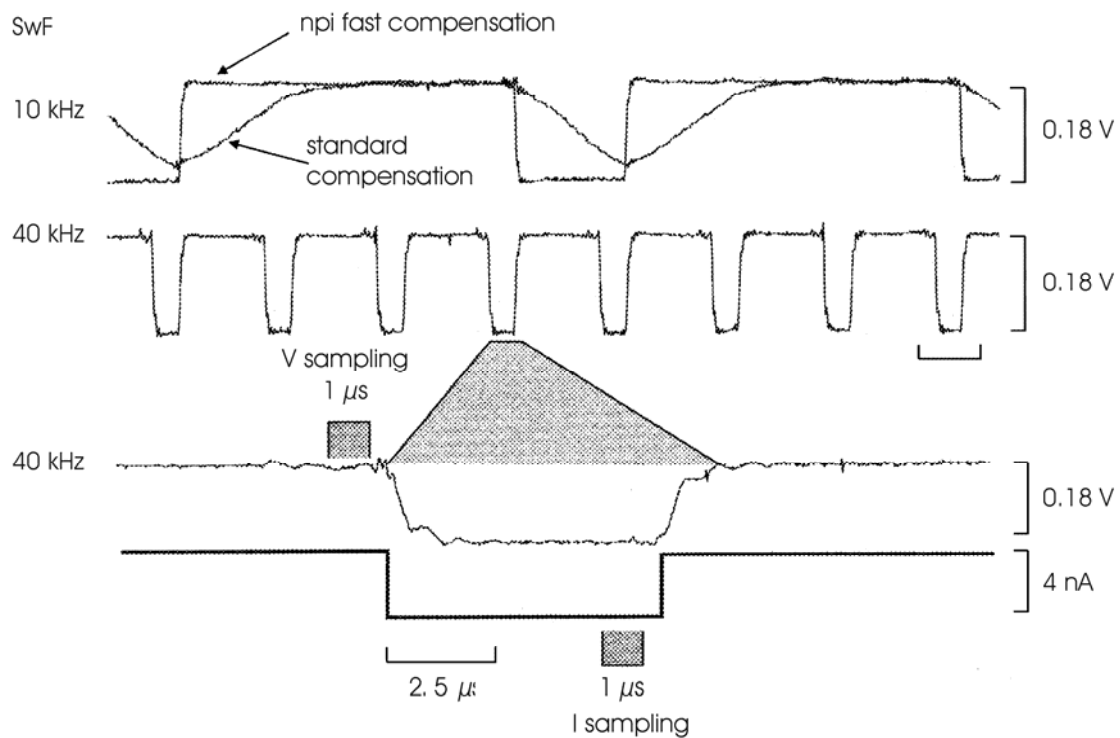


Figure 17: Microelectrode artifact settling

Compensation of stray capacities with a SEC 05 amplifier. The upper trace shows the comparison between the standard capacity compensation and the fast capacity compensation of the SEC systems. After full compensation the settling time of the microelectrode is reduced to a few microseconds allowing very high switching frequencies (here: 40 kHz, middle and lower trace). The microelectrode was immersed 3 mm deep in cerebrospinal fluid. Microelectrode resistance: 45 M $\Omega$ , current: 1 nA, duty cycle 1/4. SwF: switching frequency. Original data kindly provided by Prof. Diethelm W. Richter, Goettingen. For details see (Richter et al., 1996).

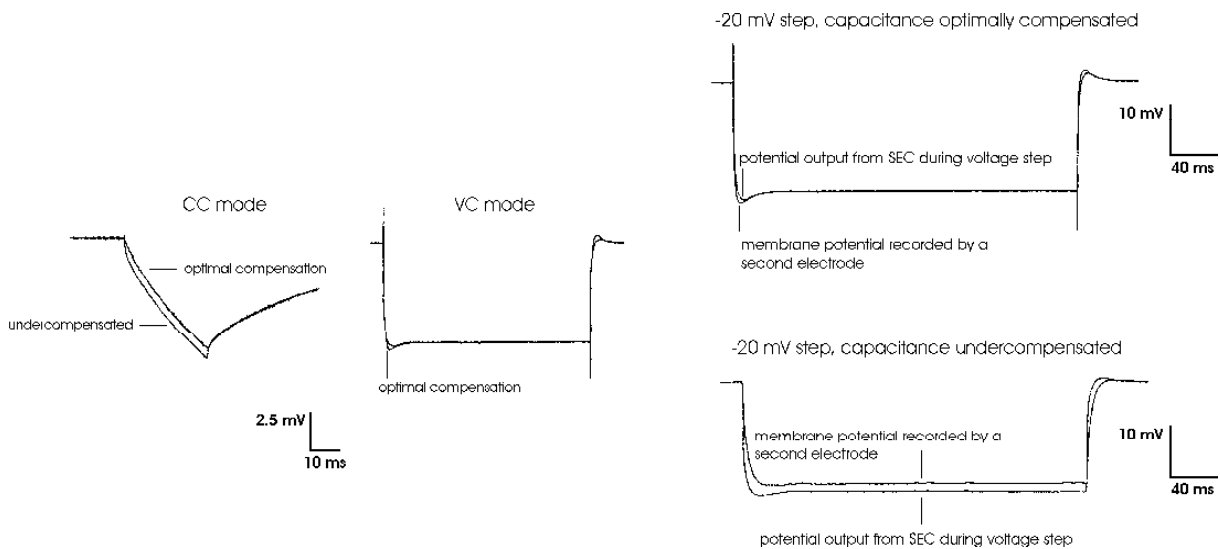


Figure 18: Errors resulting from wrong compensation of the electrode capacity. Original data kindly provided by Ajay Kapur. For details see (Kapur et al., 1998).

## 8.6. Capacity Compensation - Tuning Procedure

### *First part: basic setting*

In SEC systems the capacity compensation of the electrode is split into two controls, the coarse control at the headstage and a the fine control at the front panel of the amplifier. The aim of the first part of the tuning procedure is to set the coarse capacity compensation at the headstage, so that an optimal, wide range of C.COMP. at the amplifier is achieved.

- ❑ Insert the electrode into the electrode holder and connect it to the amplifier.
- ❑ Immerse the electrode, as deep as it will be during the experiment, into the bath solution.
- ❑ Set the C.COMP. control at the amplifier (potentiometer #24 at the front panel) to a value around 2 and turn COARSE CAPACITY COMPENSATION at the headstage to the leftmost position.
- ❑ Connect the BNC connector ELECT. POTENTIAL OUTPUT (#16 at the front panel) to an oscilloscope and trigger with the signal at BNC connector SWITCH. FREQUENCY (SYNC. OUT) (#14 at the front panel). The oscilloscope should be in external trigger mode. The time base of the oscilloscope should be in the range of 250  $\mu$ s..
- ❑ Set the amplifier in CC mode and select the lowest switching frequency (1 to 2 kHz)
- ❑ Apply positive or negative current to the electrode using the HOLD. CUR control (potentiometer #9 at the front panel).
- ❑ You should see a signal at the oscilloscope similar to those in Figure 19. Turn the COARSE CAPACITY COMPENSATION carefully clockwise until the signal becomes as square as possible (lower diagram in Figure 19).

***Important:*** If you use a model cell (e.g. to train yourself in adjusting the capacity compensation) the capacity of the model cell is always present. Thus, you will get an approximately square shaped signal with a slight slope as shown in Figure 20 (lower panel).

- ❑ Increase the switching frequency to at least 15 kHz. The amplitude and shape of the signal should not change considerably.

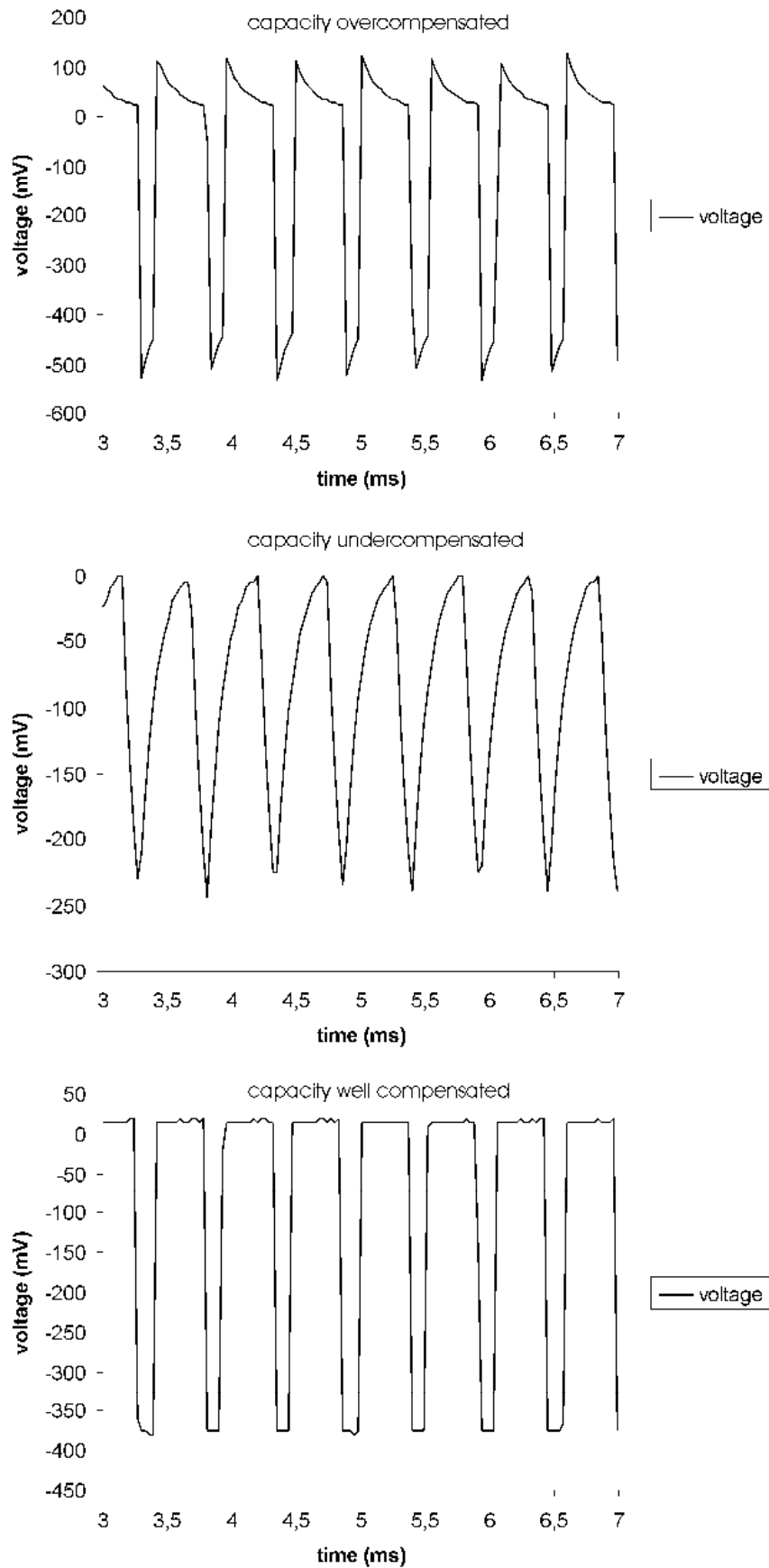


Figure 19: Tuning of the coarse capacity compensation with an electrode (resistance 100 M $\Omega$ ) in the bath. Time course of the signal at ELECTRODE POTENTIAL OUTPUT is shown (holding current: -1 nA, switching frequency: 2 kHz).

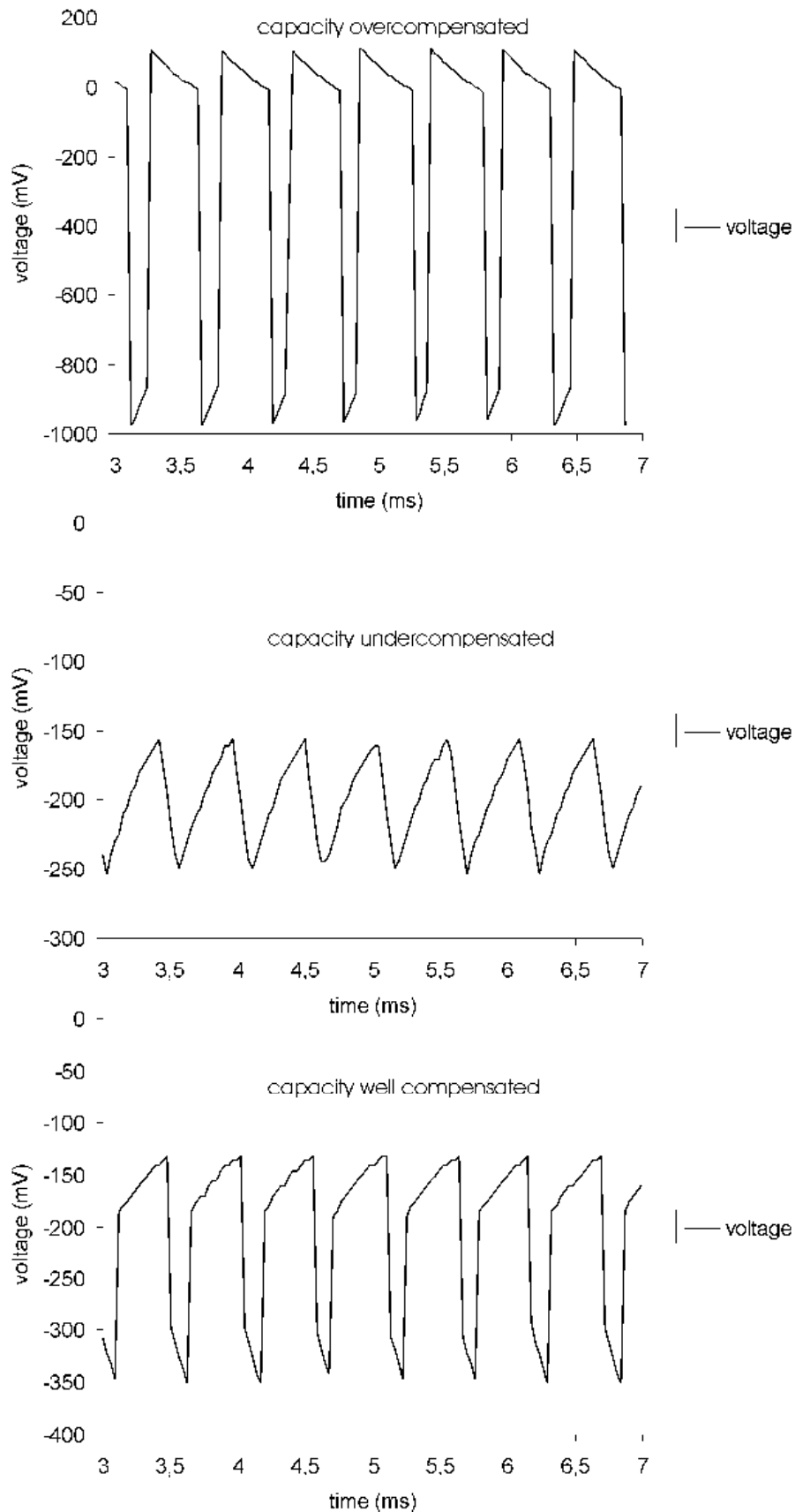


Figure 20: Tuning of the coarse capacity compensation. Time course of the signal at ELECTRODE POTENTIAL OUTPUT is shown (holding current: -1 nA, switching frequency: 2 kHz). A cell model was connected (electrode resistance 100 M $\Omega$ ).

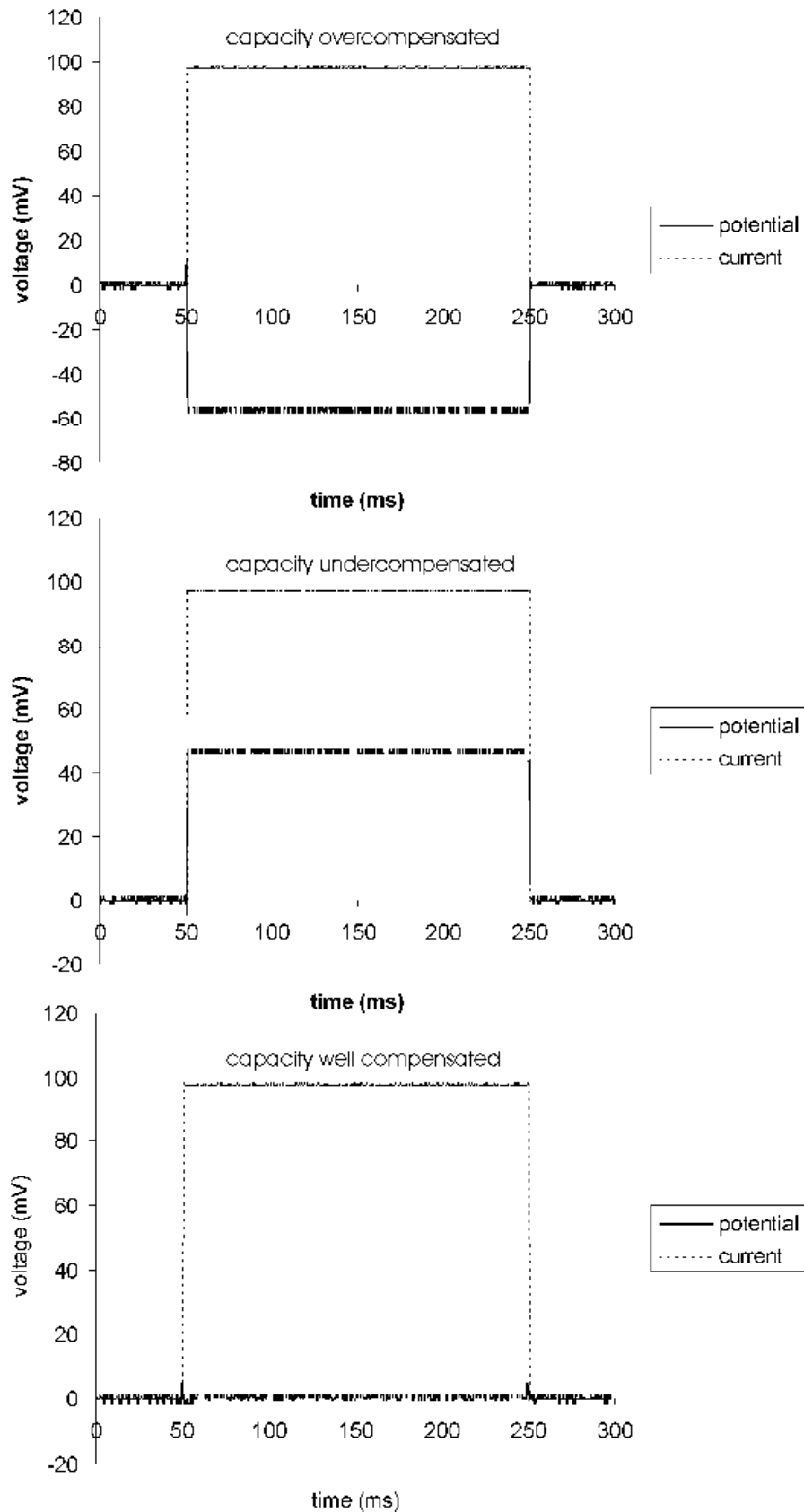


Figure 21: Capacity compensation of the electrode in the bath (electrode resistance: 100 M $\Omega$ , Current stimulus: 1 nA, switching frequency: 2 kHz). Current stimulus and electrode potential are shown.

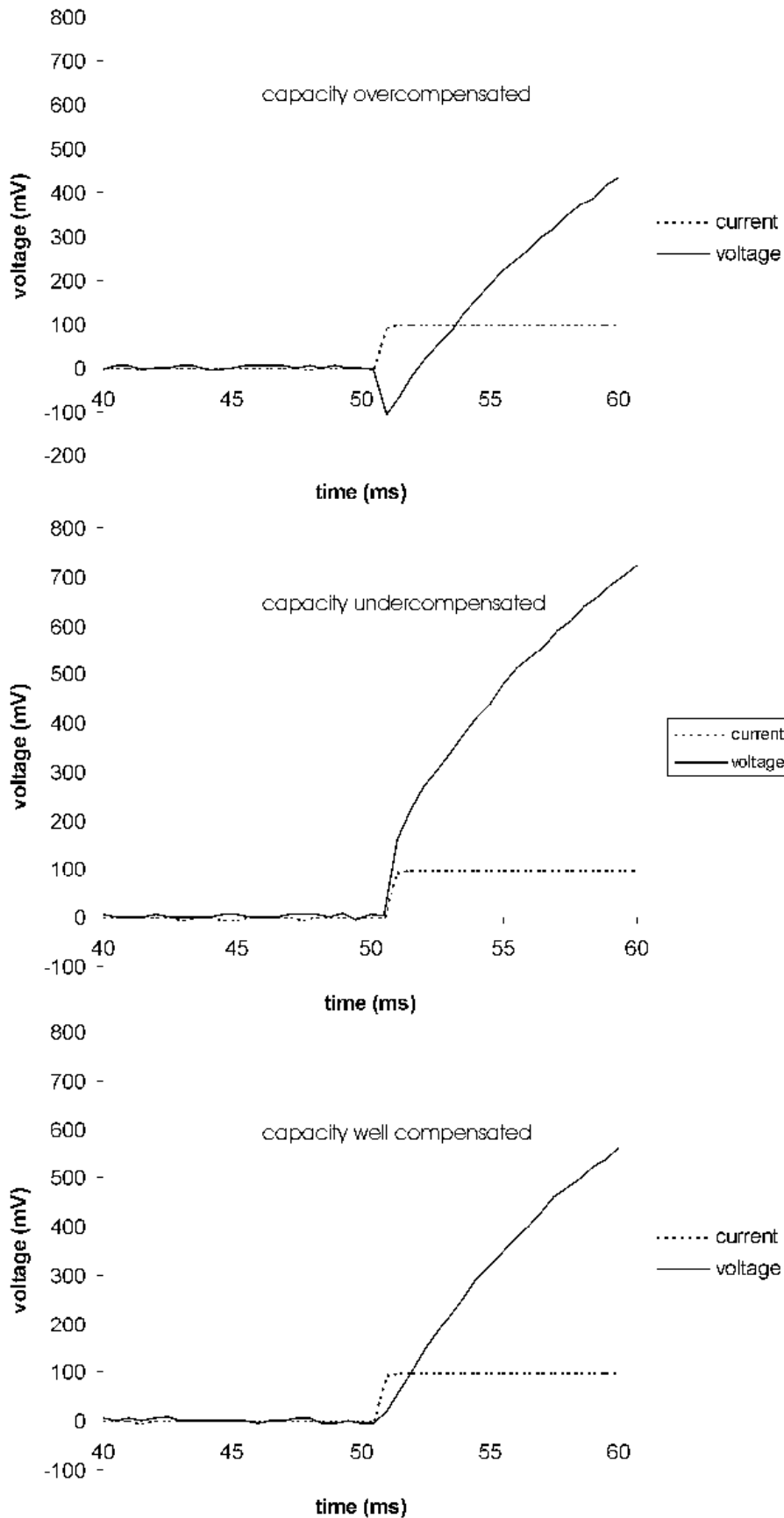


Figure 22: Capacity compensation of the electrode using a cell model (electrode resistance: 100 M $\Omega$ , current: 1 nA, cell membrane: 100 M $\Omega$ , 100 pF, switching frequency: 2 kHz). Current stimulus and membrane potential are shown.

*Second part: fine tuning*

Now the basic setting of the CAPACITY COMPENSATION is achieved. Since the electrode parameters change during the experiment (especially after impaling a cell), it is necessary to fine tune the CAPACITY COMPENSATION during the experiment using the C.COMP. control on the amplifier. To get familiar with this, connect a cell model and go through the following steps (the procedure is the identical with a “real” cell).

- ❑ Connect POTENTIAL OUTPUT and CURRENT OUTPUT (front panel) to another oscilloscope.
- ❑ Set SWITCHING FREQUENCY to the desired value (>15 kHz).
- ❑ Set the HOLDING CURRENT to zero. With the amplifier in CC mode, apply square pulses of a few nA (or a few tens of pA for patch recordings) to the cell. Negative current pulses are recommended. If you apply positive current pulses, be sure only to elicit ohmic responses of the cell membrane, i.e. pulses should not elicit openings of voltage gated channels.
- ❑ The POTENTIAL OUTPUT should show the ohmic response of the cell membrane, without an artifact, as illustrated in Figure 22 and Figure 23.

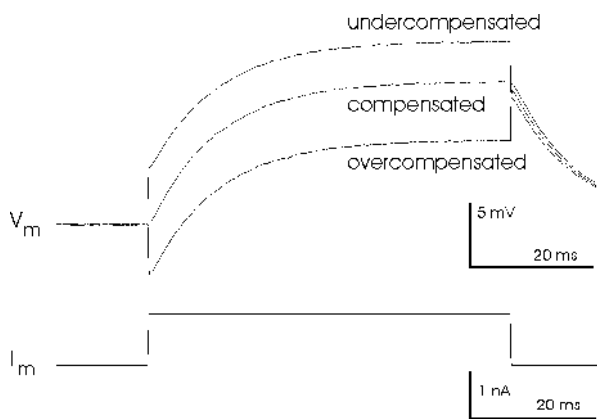


Figure 23: Capacity compensation of the electrode inside a cell (in CC mode). Current stimulus and membrane potential are shown.

***Hint:*** The results of this procedure look very similar to tuning of the bridge balance. If the BRIDGE is balanced accurately no differences in the potential outputs should occur when switching between CC- and BR mode.

***Important:*** Always monitor the OUTPUT from ELECT. POTENTIAL, using a second oscilloscope. The signals must be always square. If not, CAPACITY COMPENSATION has to be readjusted or the switching frequency must be lowered.

## 8.7. Testing Operation Modes

### *Current Clamp (in BR- or discontinuous CC mode)*

The cell's response to current injections is measured in the current clamp (CC) mode. Current injection is performed by means of a current source connected to the microelectrode. Basically the test procedure in BR and CC mode is the same. In the following it is assumed that the basic settings and the tuning procedures are carried out as described in chapters 8.1 to 8.6. All numbers refer to Figure 8.

- Connect the cell model (see.
- Set the amplifier to CC or BR mode, respectively, using the MODE OF OPERATION switch (#1).
- Set the membrane resistance of the cell model to 100 M $\Omega$  (see chapter 7).
- Set the holding current to  $-0.5$  nA using the HOLD potentiometer (#9) (setting: 50, reading:  $-0.50$  nA) and the HOLD current polarity switch (#9) to -.
- Make sure that the ELECTRODE RESISTANCE test is not active.
- The POTENTIAL display should read  $-50$  mV (according to Ohm's law). The voltage at POTENTIAL OUTPUT BNC (#17) should be  $-500$  mV.

**Remember:** The voltage at POTENTIAL OUTPUT is the membrane potential multiplied by 10!

- Apply a test pulse of 1 nA to the cell model by giving a voltage step of 0.5 V to CUR. STIM. INPUT (#12). The length of the test pulse should be at least 30 ms.
- You should see a potential step of 500 mV amplitude at POTENTIAL OUTPUT BNC (#17). Due to the membrane capacity the step is smoothed.

**Note:** If you expect the POTENTIAL display to show the value of the potential step (in this case  $+50$  mV amplitude from a "resting potential" of  $-50$  mV, i.e.  $-0$  mV) remember that the display is rather sluggish and may not display the right value (depending on the length of the step). The same is true for the CURRENT display.

### *Voltage Clamp*

In voltage clamp mode, the membrane potential is forced by a controller to maintain a certain value or to follow an external command. That allows measurement of ion fluxes across the cell membrane. This is the most complex mode of operation with the SEC-03M. Special precautions must be taken while tuning the control circuit in order avoid stability problems.

- Make sure that the amplifier works correctly with the cell model in CC mode (see above).
- Leave the membrane resistance of the cell model at 100 M $\Omega$ .
- Set the holding potential to  $-50$  mV using the HOLD potentiometer (#21, setting: 050, reading: 050 mV) and the HOLD potential polarity switch (#21) to -.
- Disable the INTEGRATOR by setting the INTEGR. switch (#20) to OFF.
- Set the GAIN (#23) to 0.1.
- Set the amplifier with the MODE OF OPERATION switch (#1) to VC mode.
- The upper display should show the holding potential of  $-50$  mV and the lower display the holding current of  $-0.5$  nA (according to Ohm's law).

***Hint:*** If the system oscillates as soon as you switch to VC mode, switch back to CC mode and check the settings. GAIN too high? CAPACITY COMPENSATION not properly adjusted, i.e. not overcompensated? INTEGRATOR switch not to OFF?

- Apply a test pulse of 20 mV to the cell model by giving a voltage step of 0.2 V to VC COMM. INPUT (#18). The length of the test pulse should be at least 30 ms.
- You should see a potential step of 200 mV amplitude at POTENTIAL OUTPUT (#17).

***Note:*** If you expect the POTENTIAL display to show the value of the potential step (in this case +20 mV amplitude from a holding potential of -50 mV, i.e. -30 mV) remember that the display is rather sluggish and may not display the right value (depending on the length of the step). The same is true for the CURRENT display.

## 9. Sample Experiments

In the following the basics of a simple experiment are described either using a sharp or a suction (patch) electrode.

It is assumed that all connections are built as described in chapter 6. Before starting remove the cell model.

### 9.1. Sample Experiment using a Sharp Microelectrode

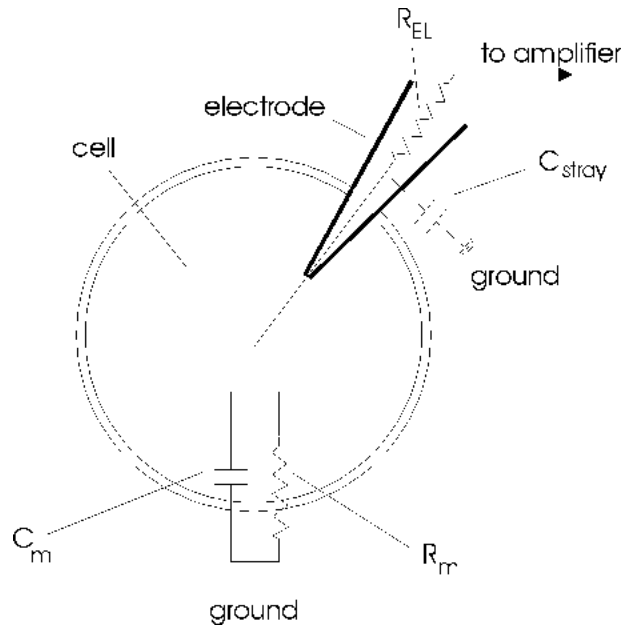


Figure 24: Model circuit for intracellular recording using a sharp electrode  
 $C_m$ : membrane capacitance,  $C_{stray}$ : electrode stray capacitance,  $R_{EL}$ : electrode resistance,  $R_m$ : membrane resistance

- Connect the electrode cable / holder to the SMB connector and the Ag-AgCl pellet or the agar-bridge for grounding the bath with GND at the headstage.
- Make the basic settings (see chapter 6).

**Again:** It is of major importance that SEC-03M systems are used only in warmed-up condition, i.e. 20 to 30 minutes after turning power on.

- Adjust BIAS CURRENT to zero if necessary (see chapter 8.1)
- Reconnect the CUR. STIM. INPUT and/or the VC COMMAND INPUT, put an electrode into the electrode holder and attach it to the headstage.
- Immerse the electrode into the bath (not in a cell) as deep as necessary during the experiment. Test the capability of the electrode to carry current (see chapter 8.2), compensate the potential offset (see chapter 8.3), compensate the input capacitance (see chapter 8.6) and measure the electrode resistance (using switch #22 , Figure 8).
- Apply current steps to the CUR. STIM. INPUT and adjust the BRIDGE BALANCE to suppress all artifacts on the POTENTIAL OUTPUT(see chapter 8.4).

- Now the system is preadjusted for measurements in BR mode. Find a cell!
  - Approach the desired cell. There are several indications that the electrode is very close to the cell membrane:
    - the electrode resistance increases (the bridge balance appears undercompensated)
    - extracellular action potentials (APs) are recorded
  - Apply a BUZZ to the electrode.
  - If you are lucky, the tip of the electrode is now inside the cell.
  - If necessary readjust BRIDGE BALANCE and/or C.COMP as shown in Figure 25 and Figure 26 using current stimuli that do not activate ion channels or transporters.
  - You read the membrane potential and can apply current pulses to the cell. After penetration the voltage responses of the cell to the test pulses should reflect the cell membrane resistance and time constant.
  - Start the experiment in BR mode
- or
- Switch to discontinuous CC mode. The shape of voltage and current traces should not change considerably.
  - If you intend to work in discontinuous VC mode, tune the system in CC mode (see above), then switch to VC mode and adjust the clamp as described in chapters 10 and 12.3.

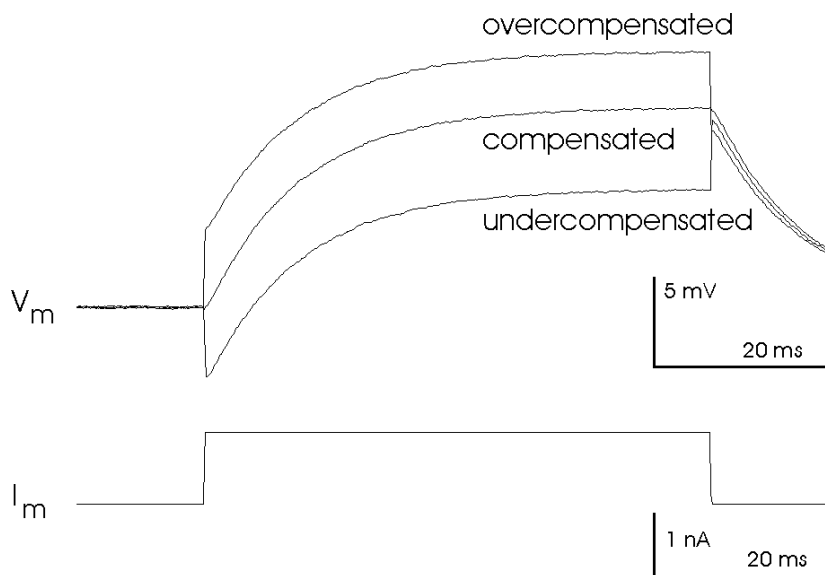


Figure 25: Adjustment of the bridge balance after penetrating a cell

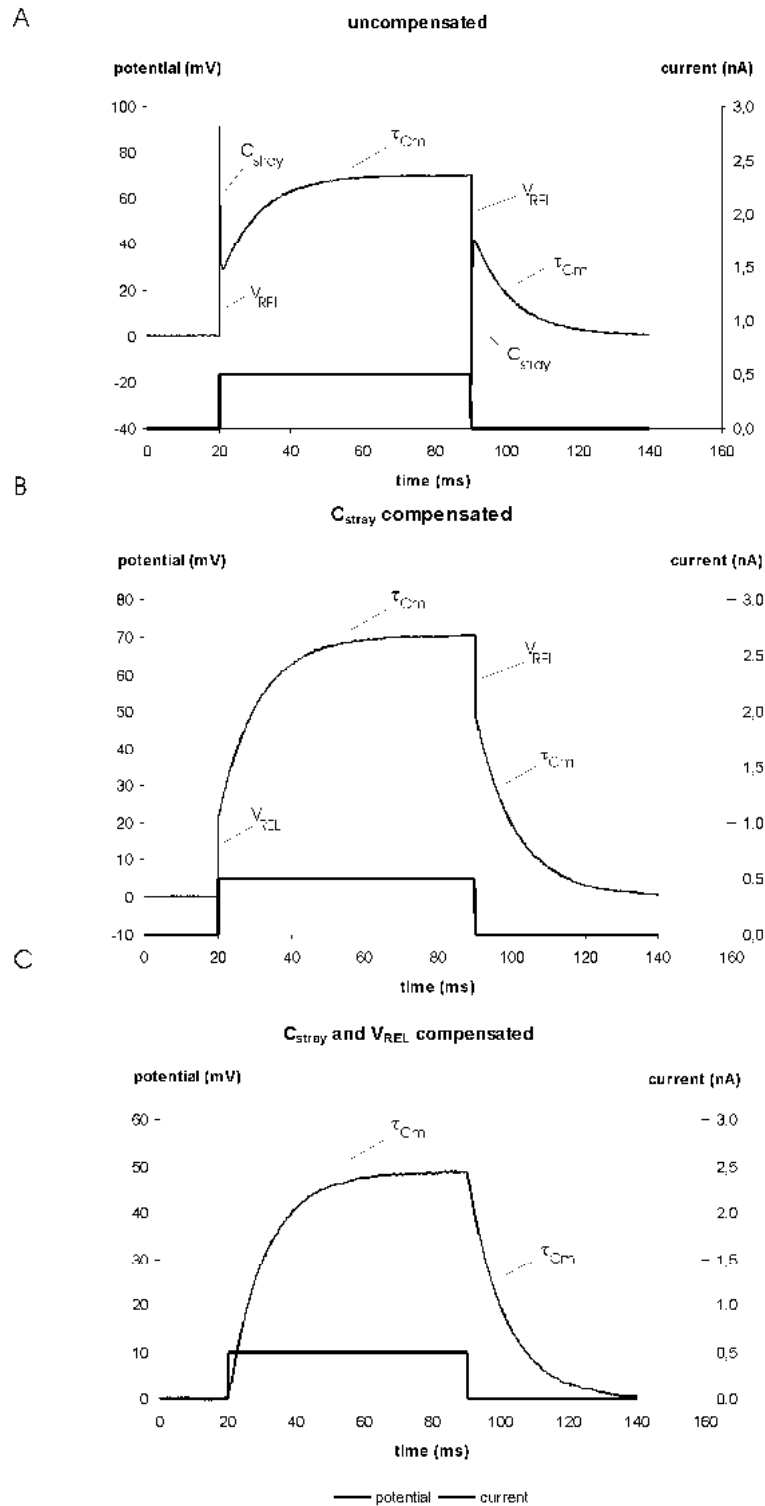


Figure 26: Artifacts caused by the recording electrode. The measurements were done in BR mode using a cell model with 100 M $\Omega$  membrane resistance, 100 pF membrane capacitance and 100 M $\Omega$  electrode resistance. **A:**  $C_{stray}$  and  $V_{REL}$  not compensated (bridge not balanced) **B:**  $C_{stray}$ : compensated and  $V_{REL}$  not compensated **C:**  $C_{stray}$  and  $V_{REL}$  compensated (bridge balanced)  $C_m$ : membrane capacitance,  $C_{stray}$ : electrode stray capacitance,  $R_{EL}$ : electrode resistance,  $R_m$ : membrane resistance,  $\tau_{Cm}$ : time constant of the cell membrane,  $V_{REL}$ : potential drop at  $R_{EL}$  (see also Figure 5)

## 9.2. Sample Experiment using a Suction Electrode

If suction electrodes are used for whole cell recordings they are usually called “pipettes”. Thus, in this subchapter “pipette” means “suction electrode”.

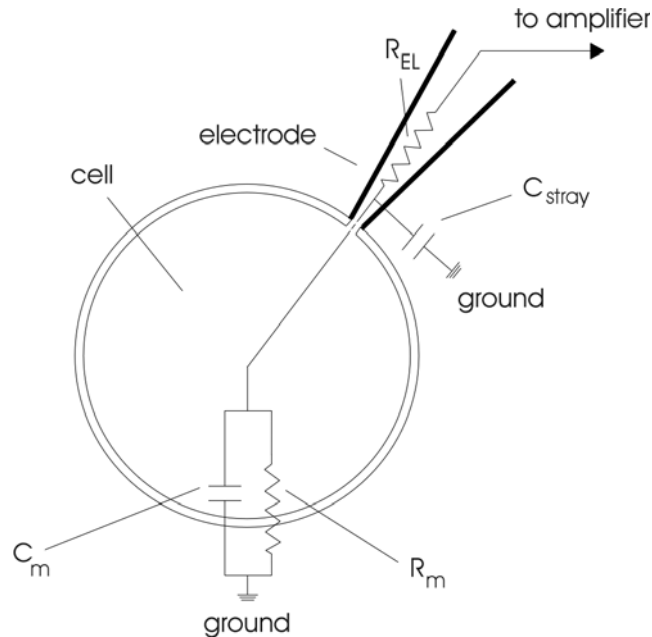


Figure 27: Model circuit for whole cell patch clamp recording using a suction electrode  
 $C_m$ : membrane capacitance,  $C_{stray}$ : electrode stray capacitance,  $R_{EL}$ : electrode resistance,  $R_m$ : membrane resistance

- ❑ Prepare the setup and proceed as described in the previous subchapter (9.1) until you have selected a cell. Before immersing the pipette into the bath apply slight positive pressure to the pipette to prevent settling of particles at the tip.
- ❑ Apply test pulses to the pipette (about 10 pA). The resulting voltage signals at the pipette are very small (50  $\mu$ V with a 5 M $\Omega$  pipette).
- ❑ Approach the cell until the voltage signal changes (**a**, Figure 28). Often you can observe a slight dent in the cell membrane.
- ❑ Release pressure from the pipette. Now forming of the seal is indicated by the voltage deflections getting much larger.
- ❑ If the seal does not form apply gentle suction to the pipette until a gigaseal is established (**b**, Figure 28).
- ❑ Apply stronger suction to the pipette or use the BUZZ unit to brake the cell membrane under the pipette opening and establish the whole cell configuration. The whole cell configuration is established if you see the voltage signal getting smaller again (**c**, Figure 28) and you read the expected membrane potential.
- ❑ Read the membrane potential and if necessary, readjust BRIDGE BALANCE and/or CAP. COMP as shown in Figure 25 and Figure 26 using current stimuli that do not activate ion channels or transporters.

❑ Start the experiment in BR mode

or

❑ Switch to discontinuous CC mode. The shape of voltage and current traces should not change considerably.

❑ If you intend to work in discontinuous VC mode, tune the system in CC mode (see above), then switch to VC mode and adjust the clamp as described in chapters 10 and 12.3.

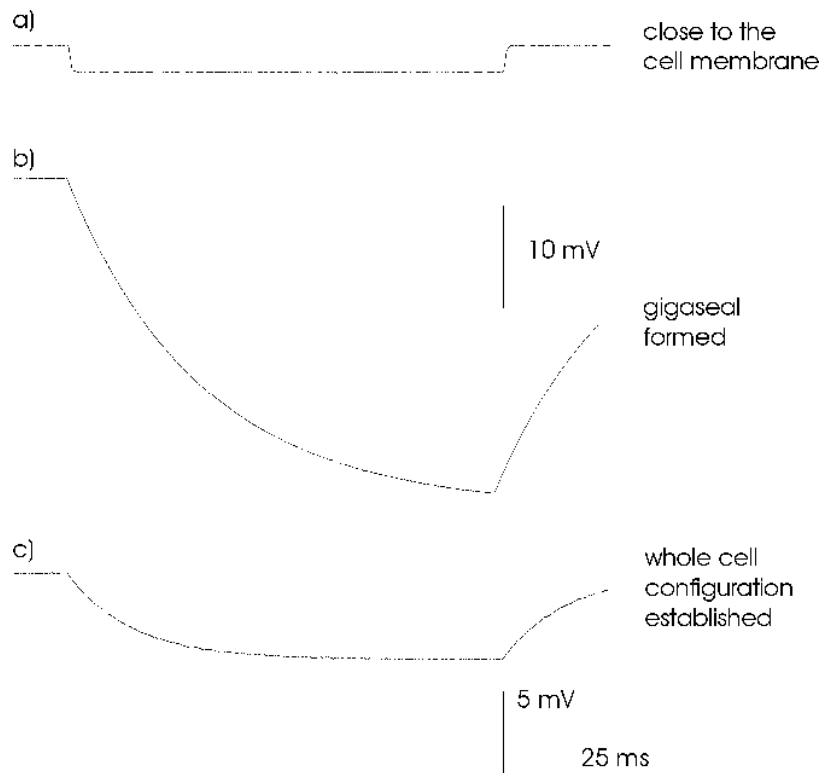


Figure 28: Approaching the cell, forming a gigaseal and establishing the whole cell configuration

## 10. Tuning VC Performance

In VC mode there is the problem that the voltage step is often not strictly angular shaped. But, for instance, increasing the clamp speed by tuning the CAPACITY COMPENSATION of the electrode or increasing GAIN also increases noise. Therefore, the settings of the different parameters result always in a compromise between the stability, accuracy, noise and control speed. In this chapter we will give some practical hints, how to optimize the accuracy and speed of the clamp. The theoretical background of adjustment criteria is discussed in chapter 11 (see also Polder and Swandulla, 2001).

The main considerations are: Do I expect rapid or slow responses to voltage changes? How much noise can I accept? Is it possible to use an electrode with low resistance?

**General:** The speed and accuracy of the voltage clamp control circuit is mainly determined by the question how much current can be injected and how fast can this happen. Thus, the more current the system can inject within a short time the better the quality of the clamp (see chapter 12.2).

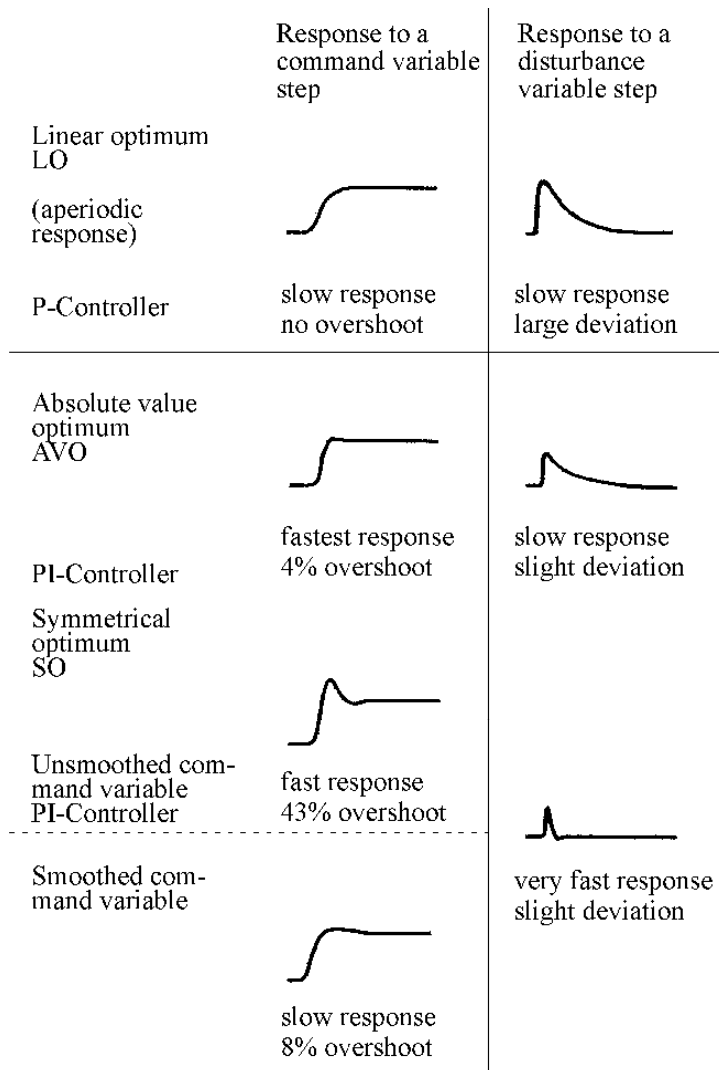
### *General Considerations*

The key to accurate and fast recording is a properly built setup.

- Make sure that the internal system ground is connected to only one point on the measuring ground and originates from the potential headstage. Multiple grounding should be avoided; all ground points should originate from a central point. The electrode used for grounding the bath should have a low resistance and must not produce offsets.
- Use electrodes with resistances as low as possible.
- Keep cables short.
- Check regularly whether cables and / or connections are broken.
- Make sure that chlorinating of silver wires for the electrodes is proper and that there are no unwanted earth bridges, e.g. salt bridges originating from experimental solutions.

SEC systems can be tuned according to one of three optimization methods (see also chapter 12.3):

1. the "linear optimum" (LO) that provides only slow response to a command step and a maximal accuracy of 90-97%.
2. the "absolute value optimum" (AVO) that provides the fastest response to a command step with very little overshoot (maximum 4%) or
3. the "symmetrical optimum" (SO) has the best performance compensating intrinsic disturbance signals but shows a considerable overshoot (maximum 43%) to a step command.



### **LO**

Only a P-Controller is used. The response to a command step is slow and has no overshoot (potential output). The response to a disturbance, e.g. an activating channel, is slow and has a large deviation.

### **AVO**

A PI-Controller is used. The response to a command step is very fast with 4% overshoot (potential output). The response to a disturbance, e.g. an activating channel, is slow and has a slight deviation.

### **SO**

A PI-Controller is used. The response to an unsmoothed command step is fast with 43% overshoot (potential output). The response to a disturbance, e.g. an activating channel, is very fast and has a slight deviation.

Figure 29: tuning VC according LO, AVO or SO. The potential output is shown.

### *Tuning Procedure*

**Important:** First use a cell model for the tuning procedure. You will get familiar with the different settings and the consequences for the system without any damage to cells or electrodes.

- Before you switch to VC mode tune all parameters related to the recording electrode (offset, capacity compensation etc.) in CC mode, set GAIN to a low, save level and turn INTEGR. (#20, Figure 8) to OFF.
- Switch to VC mode and apply identical test pulses to the cell model.
- The controller is now in P-mode (proportional only). Watch the potential output and increase the GAIN, so that no overshoot appears.
- Turn the integrator on (INTEGR., #20, Figure 8). The controller is now in PI-mode (proportional-integral). Tune the GAIN again (see above).
- Watch the potential output and tune the time constant using INTEGR., #20, Figure 8, until the overshoot of the desired tuning method appears (see also Figure 29).

## 11. Trouble Shooting

In the following section some common problems, possible reasons and their solutions are described.

***Important:*** Please note that the suggestions for solving the problems are only hints and may not work. In a complex setup it is impossible to analyze problems without knowing details. In case of trouble always contact an experienced electrophysiologist in your laboratory if possible, and connect a cell model to see whether the problem occurring with electrodes and “real” cells persists with the cell model.

### Problem 1:

After immersing an electrode into the bath there is an unusual high potential offset.

Possible reasons:

1. The Ag-AgCl coating of the silver wire in the electrode holder is damaged
2. The Ag-AgCl pellet or Ag-AgCl coating of the silver wire in the agar-bridge are damaged
3. There is an unwanted GND-bridge e.g. caused by a leaky bath
4. The headstage or the amplifier has an error

Solutions:

1. Chloride the silver wire again
2. Exchange the pellet or chloride the silver wire in the agar-bridge
3. Try to find the GND-bridge and disconnect it e.g. by sealing the bath
4. Contact npj

### Problem 2:

Even if no stimulus is given a current flows through the current electrode

Possible reason:

1. The BIAS current is not adjusted

Solution:

1. Adjust the BIAS current according the procedure described in chapter 8.1

### Problem 3:

The system oscillates (see also *voltage clamp* in chapter 8.7)

Possible reason:

1. The capacitance of the electrode is overcompensated

Solution:

1. Turn the COARSE CAPACITY COMPENSATION at the headstage and C.COMP. potentiometer (#24, Figure 8) to the most left positions and compensate the input capacitance again (see chapter 8.6)

### Problem 4:

With the cell model connected the REL display does not show the correct value (within a tolerance of 2%).

Possible reason:

1. Electrode capacity is not well compensated
2. The headstage has an error

Solution:

1. Turn the COARSE CAPACITY COMPENSATION at the headstage and C.COMP. potentiometer (#24, Figure 8) to the most left positions and compensate the input capacitance again (see chapter 8.6)
2. Contact npj

## 12. Appendix

### 12.1. Theory of Operation

Voltage clamp instruments are closed loop control systems with two inputs external to the control loop. An electronic feedback network is used to force the membrane potential of a cell to follow a voltage command (setpoint input) as fast and as accurately as possible in the presence of incoming disturbances (disturbance input, correlated with the activities of the cell e.g. activation of ion channels). This is achieved by injecting an adequate amount of charge into the cell. The current injected by the clamp instrument is a direct measure of the ionic fluxes across the membrane (Ferreira et al., 1985; Jack et al., 1975; Ogden, 1994; Smith et al., 1985).

The performance evaluation and optimal tuning of these systems can be done by considering only the command input since the mathematical models (setpoint transfer function and the disturbance transfer function, see Froehr, 1985; Polder, 1984; Polder and Swandulla, 1990; Polder, 1993; Polder and Houamed, 1994; Polder and Swandulla, 2001) are closely related. Modern control theory provides adequate solutions for the design and the optimal tuning of feedback systems (Froehr, 1985).

Most voltage clamp systems are composed only of delay elements, i.e. elements which react with a retardation to a change. This type of closed loop systems can be optimized easily by adequate shaping of the "frequency characteristic magnitude" ( $|F(j\omega)|$ ) of the associated transfer function  $F(s)$  (output to input ratio in the frequency domain = *LAPLACE* transform of the differential equation of the system, Polder and Swandulla, 2001).

Using controllers with a proportional-integral characteristic (PI-controllers) it is possible to force the magnitude of the frequency characteristic to be as close as possible to one over a wide frequency range ("modulus hugging", see Froehr, 1985; Polder and Swandulla, 1990; Polder, 1993; Polder and Houamed, 1994; Polder and Swandulla, 2001). For voltage clamps, this means that the controlled membrane potential rapidly reaches the desired command value.

The PI-controller yields an instantaneous fast response to changes (proportional gain) while the integral part increases the accuracy by raising the gain below the corner frequency of the integrator (i.e. for slow signals) to very high values (theoretically to infinite for DC signals, i.e. an error of 0%) without affecting the noise level and stability. Since the integrator induces a 0 in the transfer function, the clamp system will tend to overshoot if a step command is used. Therefore the tuning of the controller is performed following optimization rules which yield a well defined system performance (AVO and SO, see below).

The various components of the clamp feedback electronics can be described as first or second order delay elements with time constants in the range of microseconds. The cell capacity can be treated as an integrating element with a time constant  $T_m$  which is always in the range of hundreds of milliseconds.

Compared to this "physiological" time constant the "electronic" time constants of the feedback loop can be considered as "small" and added to an equivalent time constant  $T_e$ . The ratio of the "small" and the "large" time constant determines the maximum gain which can be achieved without oscillations and thus, the accuracy of the clamp. With the gain adjusted to this level the integrator time constant and "small" time constant determine the speed of response of the system.

The clamp performance can be increased considerably if the influence of the current injecting electrode is excluded as far as possible from the clamp loop since the electrode resistance is nonlinear. This is achieved if the output of the clamp system is a current source rather than a voltage source. In this case the clamp transfer function has the magnitude of a conductance (A/V). Another advantage of this arrangement is, that the clamp current can be determined by a differential amplifier with no need of virtual ground.

### 12.2. Speed of Response of SEC Single Electrode Clamps

The maximum speed of response of any clamp system to a voltage command step is determined by the cell capacity, the resistance of the current injecting electrode and the maximum output voltage of the VC amplifier (Polder and Houamed, 1994):

$$(dU_m/dt)_{max} = U_{max}/C_m * R_{el} \quad (1) \quad 1 \text{ V / s} = 10^{-3} \text{ mV / } \mu\text{s} \quad (1a)$$

The standard headstages of the SEC amplifiers are equipped with a current source output with a calibration of 10 nA / V. Therefore with a voltage of  $\pm 12$  V (linear range of the current source) a maximum current of  $\pm 120$  nA can be injected into a load of maximum 100 M $\Omega$ . In the switched CC or VC modes the maximum current has to be multiplied with the duty cycle (1/8, 1/4, or 1/2). The maximum current is 15 nA, 30 nA or 60 nA.

**Remember:** The duty cycle of the modular SEC-03M is fixed to 1/4.

With the maximum current determined electronically by the current source (for  $R_{el} < 100 \text{ M}\Omega$ ) the maximum speed of response can be calculated as:

$$(dU_m/dt)_{max} = i_{max}/C_m \quad (2)$$

For a given command step  $U_{com}$  the shortest time  $t_r$  to reach this level can be calculated as:

$$t_r = U_{com}/(dU_m/dt)_{max} \quad (3a)$$

The maximum voltage change  $\Delta U_{max}$  which can be achieved in a given period of time  $\Delta t$  is:

$$\Delta U_{max} = ((dU_m/dt)_{max} * \Delta t) \quad (3b)$$

**Examples:**

$C_m = 300 \text{ pF}$ ,  $R_m = 50\text{-}100 \text{ M}\Omega$ , (a)  $R_{el} = 5 \text{ M}\Omega$ , (b)  $R_{el} = 100 \text{ M}\Omega$

Equation (2):	$(dU_m/dt)_{max} =$	0.05mV/ $\mu$ s duty cycle = 1/8
		0.1 mV/ $\mu$ s duty cycle = 1/4
		0.2 mV/ $\mu$ s duty cycle = 1/2
Equation (3a):	$t_r =$	1 ms duty cycle = 1/8
( $U_{com} = 50 \text{ mV}$ )		0.5 ms duty cycle = 1/4
		0.25 ms duty cycle = 1/2

### 12.3. Tuning Procedures for VC Controllers

The initial settings using GAIN only guarantee only a stable clamp that is not very accurate and insufficiently rapid for certain types of experiments, e.g. investigation of fast voltage-activated ion channels or gating currents. Thus, for successful and reliable experiments, it is necessary to tune the clamp loop.

It depends on the type of experiment to which method one should follow (see below).

- “Linear Optimum” (LO)

with this method only the proportional part (GAIN) of the PI controller is used. The response to a command step is slow, but produces no overshoot. The response to a disturbance is also slow with a large deviation of the membrane potential. Clamp accuracy is maximum of 90-97% (Finkel and Redman, 1985). Therefore, this method should only be used only if it is very important to avoid overshoots of the membrane potential.

- "Absolute Value Optimum" (AVO)

uses the PI controller and provides the fastest response to a command step with very little overshoot (maximum 4%). The response to a disturbance is of moderate speed and the amplitude of the deviation is only half the amplitude obtained with LO. It is applied if maximum speed of response to a command step is desirable, e.g. if large voltage activated currents are investigated.

- "Symmetrical Optimum" (SO)

uses also the PI controller and has the best performance compensating intrinsic disturbance signals. The response to a command step shows a very steep rise phase followed by a considerable overshoot (maximum 43%). The response to a disturbance is fast and the amplitude of the deviation is in the same range as with the AVO method. The overshoot can be reduced by adequate shaping of the command pulse by a delay unit (Froehr, 1985; Polder and Swandulla, 1990; Polder and Swandulla, 2001). This method is preferred for slowly activating currents, such as those evoked by agonist application.

The upper speed limit for all optimization methods is determined by the maximum amount of current which the clamp system can force through a given electrode (see chapter 12.2).

### *Practical Implications*

In the following some practical implications of the theory discussed earlier in this chapter are outlined. It is assumed that the system is in VC mode with integrator turned OFF.

Although most of the parameters of the control chain are not known during an experiment, it is possible to tune the clamp controller by optimizing the response to a test pulse applied to the VC COMM. INPUT. The main criterion of tuning is the overshoot seen at the potential output. Since the SO method provides the tightest control it will be most sensitive to parameter settings and requires most experience.

**Note:** The transitions between the optimization methods are blurred and the tuning procedure is adapted to the experimental requirements. Often, the adequate tuning of a clamp system can be tested by specific test signals (e.g. stimulus evoked signals, etc.).

---

**Very important:** All parameters that influence clamp performance (microelectrode offset, capacity compensation, etc.) must be optimally tuned before starting the PI controller tuning procedure.

The tuning procedure involves the following steps:

**Again:** The main criterion of tuning is the amount of overshoot seen at the potential output.

Tuning of the proportional gain

- Use the command input without smoothing and apply adequate, identical pulses to the cell (e.g. small hyperpolarizing pulses).
- The controller is in P-mode (proportional only). Watch the potential output and rise the GAIN so that no overshoot appears (LO method). The response to a command step is slow and has no overshoot (potential output). The response to a disturbance, e.g. synaptic input or an activating channel, is slow and has a large deviation.

Since the integral part of the controller is disconnected a steady state error in the range of a few percents will be present.

Tuning the integrator

- Reconnect the integrator to form the complete PI controller by turning the INTEGR. potentiometer (#20, Figure 8) on.
- Apply adequate test pulses without filtering.
- Adjust the integrator time constant (#20, Figure 8) to achieve the overshoot of the selected optimization method (4% with the AVO method and 43 % with the SO method). With the AVO method the response to a command step is very fast with 4% overshoot (potential output). The response to a disturbance, e.g. an activating channel, is slow and has a slight deviation. With the SO method the response to an unsmoothed command step is fast with 43% overshoot (potential output). The response to a disturbance, e.g. an activating channel, is very fast and has a slight deviation.

Now the steady-state error must disappear.

**Note:** If the SO is used, an external command input filter can be used to smooth the command signal and consequently reduce the overshoot according to the requirements of the experiment (see also Figure 29).

## 13. Literature about npi single electrode clamp amplifiers

### 13.1. Paper in Journals

#### Recording Methods and Voltage Clamp Technique

- ❑ Dietzel, I. D., Bruns, D., Polder, H. R. and Lux, H. D. (1992). Voltage Clamp Recording, in Kettenmann, H. and R. Grantyn (eds.) *Practical Electrophysiological Methods*, Wiley-Liss, NY.
- ❑ **Lalley, P. M., Moschovakis, A. K. and Windhorst, U. (1999). Electrical Activity of Individual Neurons in Situ: Extra- and Intracellular Recording, in: U. Windhorst and H. Johansson (eds.) *Modern Techniques in Neuroscience Research*, Springer, Berlin, New York**
- ❑ Misgeld, U., Müller, W. and Polder, H. R. (1989). Potentiation and Suppression by Eserine of Muscarinic Synaptic Transmission in the Guinea-Pig Hipocampal Slice. *J.Physiol.*, **409**, 191-206.
- ❑ Polder, H. R. and Swandulla, D. (2001). The use of control theory for the design of voltage clamp systems: a simple and standardized procedure for evaluating system parameters. *J.Neurosci.Meth.* **109**, 97-109.
- ❑ Richter, D. W., Pierrefiche, O., Lalley, P. M. and Polder, H. R. (1996). Voltage-clamp analysis of neurons within deep layers of the brain. *J.Neurosci.Meth.* **67**, 121-131.
- ❑ Sutor, B., Grimm, C., & Polder, H. R. (2003). Voltage-clamp-controlled current-clamp recordings from neurons: an electrophysiological technique enabling the detection of fast potential changes at preset holding potentials. *Pflugers Arch.* **446**, 133-141.

#### Selection of switching frequency, electrode time constant, capacity compensation

- ❑ Juusola, M. (1994). Measuring complex admittance and receptor current by single electrode voltage-clamp. *J.Neurosci.Meth.* **53**, 1-6.
- ❑ Torkkeli, P. H. & French, A. S. (1994). Characterization of a transient outward current in a rapidly adapting insect mechanosensory neuron. *Pflugers Arch.* **429**, 72-78.
- ❑ Weckström, M, Kouvaleinen, E. and Juusola, M. (1992). Measurement of cell impedance in frequency domain using discontinuous current clamp and white-noise modulated current injection. *Pflugers Arch.* **421**, 469-472.

#### Dynamic Hybrid Clamp

- ❑ Dietrich, D., Clusmann, H. and T. Kral (2002). Improved hybrid clamp: resolution of tail currents following single action potentials. *J.Neurosci.Meth.* **116**, 55-63.

#### Voltage-clamp-controlled current-clamp

- ❑ Schubert, D., Kotter, R., Luhmann, H. J., & Staiger, J. F. (2006). Morphology, electrophysiology and functional input connectivity of pyramidal neurons characterizes a genuine layer va in the primary somatosensory cortex. *Cereb Cortex.* **16**, 223-236.

**Comparison of recording methods (sharp electrode, whole cell, perforated patch)**

- ❑ Jarolimek, W. and Miseld, U. (1993). 4-Aminopyridine-induced synaptic GABA-B currents in granule cells of the guinea-pig hippocampus. *Pflügers Arch.* **425**, 491-498.
- ❑ Kapur, A., Yeckel, M. F., Gray, R. and Johnston, D. (1998). L-Type calcium channels are required for one form of hippocampal mossy fiber LTP. *J.Neurophysiol.* **79**, 2181-2190.
- ❑ Magistretti, J., Mantegazza, M., Guatteo, E. and Wanke, E. (1996). Action potentials recorded with patch-clamp amplifiers: are they genuine? *Trends Neurosci.* **19**, 530-534.

**Recordings of fast Na<sup>+</sup> channels**

- ❑ Inceoglu, A. B., Hayashida, Y., Lango, J., Ishida, A. T., & Hammock, B. D. (2002). A single charged surface residue modifies the activity of ikitoxin, a beta-type Na<sup>+</sup> channel toxin from *Parabuthus transvaalicus*. *Eur.J Biochem.* **269**, 5369-5376.
- ❑ Hayashida, Y., Partida, G. J., & Ishida, A. T. (2004). Dissociation of retinal ganglion cells without enzymes. *J Neurosci.Methods* **137**, 25-35.
- ❑ Hayashida, Y. & Ishida, A. T. (2004). Dopamine receptor activation can reduce voltage-gated Na<sup>+</sup> current by modulating both entry into and recovery from inactivation. *Journal of Neurophysiology* **92**, 3134-3141.

**Coating of sharp microelectrodes for VC recordings**

- ❑ Juusola, M., Seyfarth E. A. and French, A. S. (1997). Fast coating of glass-capillary microelectrodes for single-electrode voltage clamp, *J.Neurosci.Meth.* **71**, 199-204.

**Recordings with high resistance (150-220 MΩ) sharp microelectrodes**

- ❑ Highstein, S. M., Rabbitt, R. D., Holstein, G. R., & Boyle, R. D. (2005). Determinants of spatial and temporal coding by semicircular canal afferents. *J.Neurophysiol.* **93**, 2359-2370.
- ❑ Niven, J. E., Vahasoyrinki, M., Kauranen, M., Hardie, R. C., Juusola, M., & Weckstrom, M. (2003). The contribution of Shaker K<sup>+</sup> channels to the information capacity of *Drosophila* photoreceptors. *Nature* **421**, 630-634.
- ❑ Rabbitt, R. D., Boyle, R., Holstein, G. R., & Highstein, S. M. (2005). Hair-cell versus afferent adaptation in the semicircular canals. *Journal of Neurophysiology* **93**, 424-436.
- ❑ Wolfram, V. & Juusola, M. (2004). The Impact of Rearing Conditions and Short-Term Light Exposure on Signaling Performance in *Drosophila* Photoreceptors. *Journal of Neurophysiology* **92**, 1918-1927.

**Capacitive transients in VC recordings**

- ❑ Sutor, B., Hablitz, J. J. (1989). Excitatory postsynaptic potentials in rat neocortical neurons in vitro. I. Electrophysiological evidence for two distinct EPSPs. *J.Neurophysiol.* **61**, 607-620.

**Leak subtraction**

- ❑ Sutor, B., Zieglgänsberger, W. (1987). A low-voltage activated, transient calcium current is responsible for the time-dependent depolarizing inward rectification of rat neocortical neurons in vitro. *Pflügers Arch.* **410**, 102-111.

### Double cell voltage clamp method

- ❑ Dhein, St. (1998). *Cardiac Gap Junction Channels, Physiology, Regulation, Pathophysiology and Pharmacology*, Karger, Basel.

### Double Cell Recordings / Gap Junctions

- ❑ Bedner, P., Niessen, H., Odermatt, B., Willecke, K., & Harz, H. (2003). A method to determine the relative cAMP permeability of connexin channels. *Exp.Cell Res.* **291**, 25-35.
- ❑ Bedner, P., Niessen, H., Odermatt, B., Kretz, M., Willecke, K., & Harz, H. (2005). Selective permeability of different connexin channels to the second messenger cyclic AMP. *J Biol.Chem.*
- ❑ Dhein, S., Wenig, S., Grover, R., Tudyka, T., Gottwald, M., Schaefer, T. & Polontchouk, L. (2002) Protein kinase Calpha mediates the effect of antiarrhythmic peptide on gap junction conductance. *Cell Adhes Commun*, **8**, 257-264.
- ❑ Dupont, E., Hanganu, I. L., Kilb, W., Hirsch, S., & Luhmann, H. J. (2006). Rapid developmental switch in the mechanisms driving early cortical columnar networks. *Nature.* **439**, 79-83.
- ❑ Müller, A., Lauven, M., Berkels, R., Dhein, S., Polder, H. R. and Klaus, W. (1999). Switched single electrode amplifiers allow precise measurement of gap junction conductance. *Amer.J.Physiol. (Cell)* **276** (4), C980-C988.
- ❑ Polontchouk, L., Ebelt, B., Jackels, M., & Dhein, S. (2002). Chronic effects of endothelin 1 and angiotensin II on gap junctions and intercellular communication in cardiac cells. *FASEB J* **16**, 87-89.
- ❑ Weng, S., Lauven, M., Schaefer, T., Polontchouk, L., Grover, R. & Dhein, S. (2002) Pharmacological modification of gap junction coupling by an antiarrhythmic peptide via protein kinase C activation. *FASEB J.*, **16**, 1114-1116.
- ❑ Xing, D., Kjolbye, A. L., Nielsen, M. S., Petersen, J. S., Harlow, K. W., Holstein-Rathlou, N. H., & Martins, J. B. (2003). ZP123 increases gap junctional conductance and prevents reentrant ventricular tachycardia during myocardial ischemia in open chest dogs. *J Cardiovasc.Electrophysiol.* **14**, 510-520.

### Simultaneous recordings with two SEC amplifiers

- ❑ Haag, J. and Borst, A. (1996). Amplification of high-frequency synaptic inputs by active dendritic membrane processes. *Nature* **379**, 639-641.
- ❑ Haag, J. and Borst, A. (2001). Recurrent Network Interactions Underlying Flow-Field Selectivity of Visual Interneurons. *J.Neurosci* **21** (15), 5685–5692.
- ❑ Haag, J. and Borst, A. (2002). Dendro-Dendritic Interactions between Motion-Sensitive Large-Field Neurons in the Fly. *J.Neurosci* **22** (8), 3227–3233.
- ❑ Haag, J. & Borst, A. (2004). Neural mechanism underlying complex receptive field properties of motion-sensitive interneurons. *Nat.Neurosci* **7**, 628-634.

### Simultaneous intracellular recordings during voltammetric measurements

- ❑ Kudernatsch, M., Sutor, B. (1994). Cholinergic modulation of dopamine overflow in the rat neostriatum: a fast cyclic voltammetric study in vitro. *Neurosci. Letters* **181**, 107-112.
- ❑ Schlösser, B., Kudernatsch, M. B., Sutor, B. and ten Bruggencate, G. (1995). d -, m - and k -opioid receptor agonists inhibit dopamine overflow in rat neostriatal slices. *Neurosci. Letters* **191**, 126-130.

**Intra- and extracellular drug application during single electrode clamping**

- ❑ Scuvee-Moreau, J., Liegeois, J. F., Massotte, L., & Seutin, V. (2002). Methyl-laundanosine: a new pharmacological tool to investigate the function of small-conductance Ca(2+)-activated K(+) channels. *J Pharmacol.Exp.Ther.* **302**, 1176-1183.
- ❑ Dutschmann, M., Bischoff, M., Busselberg, D., & Richter, W. (2003). Histaminergic modulation of the intact respiratory network of adult mice. *Pflugers Arch.* **445**, 570-576.
- ❑ Eder, M., Becker, K., Rammes, G., Schierloh, A., Azad, S. C., Zieglgansberger, W., & Dodt, H. U. (2003). Distribution and Properties of Functional Postsynaptic Kainate Receptors on Neocortical Layer V Pyramidal Neurons. *J Neurosci.* **23**, 6660-6670.
- ❑ Hanganu, I. L., Kilb, W. and Luhmann, H. J. (2001). Spontaneous synaptic activity of subplate neurons in neonatal rat somatosensory cortex. *Cerebral Cortex* **11** (5), 400-410.
- ❑ Hanganu, I. L. & Luhmann, H. J. (2004). Functional nicotinic acetylcholine receptors on subplate neurons in neonatal rat somatosensory cortex. *Journal of Neurophysiology* **92**, 189-198.
- ❑ Heck, N., Kilb, W., Reiprich, P., Kubota, H., Furukawa, T., Fukuda, A., & Luhmann, H. J. (2006). GABA-A Receptors Regulate Neocortical Neuronal Migration In Vitro and In Vivo. *Cereb Cortex*. doi:10.1093/cercor/bhj135
- ❑ Lalley, P. M. (1999). Microiontophoresis and Pressure Ejection, in: U. Windhorst, and H. Johansson (eds) *Modern Techniques in Neuroscience Research*, Springer, Berlin, New York.
- ❑ Lalley, P. M., A. K. Moschovakis and U. Windhorst (1999). Electrical Activity of Individual Neurons in Situ: Extra- and Intracellular Recording, in: U. Windhorst and H. Johansson (eds.) *Modern Techniques in Neuroscience Research*, Springer, Berlin, New York.
- ❑ Lalley, P. M. (2003). {micro}-Opioid receptor agonist effects on medullary respiratory neurons in the cat: evidence for involvement in certain types of ventilatory disturbances. *Am.J Physiol Regul.Integr.Comp Physiol* **285**, R1287-R1304.
- ❑ Ponimaskin, E., Dumuis, A., Gaven, F., Barthet, G., Heine, M., Glebov, K., Richter, D. W., & Oppermann, M. (2005). Palmitoylation of the 5-Hydroxytryptamine4a Receptor Regulates Receptor Phosphorylation, Desensitization, and {beta}-Arrestin-Mediated Endocytosis. *Molecular Pharmacology* **67**, 1434-1443.
- ❑ Richter, D. W., Pierrefiche, O., Lalley, P. M. & Polder, H. R. (1996). Voltage-clamp analysis of neurons within deep layers of the brain. *J.Neurosci.Meth.* **67**, 121-131.
- ❑ Schubert, D., Staiger, J. F., Cho, N., Koetter, R., Zilles, K. and Luhmann, H. J. (2001). Layer-Specific Intracolumnar and Transcolumnar Functional Connectivity of Layer V Pyramidal Cells in Rat Barrel Cortex. *J.Neurosci* **21** (10), 3580–3592.
- ❑ Schubert, D., Kotter, R., Zilles, K., Luhmann, H. J., & Staiger, J. F. (2003). Cell Type-Specific Circuits of Cortical Layer IV Spiny Neurons. *J Neurosci.* **23**, 2961-2970.
- ❑ Schubert, D., Kotter, R., Luhmann, H. J., & Staiger, J. F. (2005). Morphology, Electrophysiology and Functional Input Connectivity of Pyramidal Neurons Characterizes a Genuine Layer Va in the Primary Somatosensory Cortex. *Cerebral Cortex* bhi100.
- ❑ Weiss, T., Veh, R. W., & Heinemann, U. (2003). Dopamine depresses cholinergic oscillatory network activity in rat hippocampus. *Eur.J Neurosci.* **18**, 2573-2580.

### Tracer injection and intracellular recording

- ❑ Poulet, J. F. & Hedwig, B. (2006). The cellular basis of a corollary discharge. *Science*. **311**, 518-522.
- ❑ Röhrig, G., Klaus, G., & Sutor, B. (1996). Intracellular acidification reduced gap junction coupling between immature rat neocortical pyramidal neurons. *J.Physiol.* **490** (1), 31-49.

### Visualization, imaging and infrared video microscopy

- ❑ Dodt, H. U and Zieglgänsberger, W. (1994). Infrared videomicroscopy: a new look at neuronal structure and function, *Trends in Neurosciences*, **19** (11), 453-458.
- ❑ Haag, J., Denk, W., & Borst, A. (2004). Fly motion vision is based on Reichardt detectors regardless of the signal-to-noise ratio. *Proc.Natl.Acad.Sci.U.S.A* **101**, 16333-16338.
- ❑ Jacob, S. N., Choe, C. U., Uhlen, P., DeGray, B., Yeckel, M. F., & Ehrlich, B. E. (2005). Signaling microdomains regulate inositol 1,4,5-trisphosphate-mediated intracellular calcium transients in cultured neurons. *Journal of Neuroscience* **25**, 2853-2864.
- ❑ Kapur A., M. Yeckel and Johnston, D. (2001). Hippocampal mossy fiber activity evokes Ca<sup>2+</sup> release in CA3 pyramidal neurons via a metabotropic glutamate receptor pathway. *Neuroscience* **107** (1), 59-69.
- ❑ Single, S. and Borst, A. (1998). Dendritic Integration and Its Role in Computing Image Velocity. *Science* **281**, 1848-50.
- ❑ Single, S. and Borst, A. (2002) Different Mechanisms of Calcium Entry Within Different Dendritic Compartments. *J.Neurophysiol.* **87**, 1616–1624.
- ❑ Schierloh, A., Eder, M., Zieglgansberger, W., & Dodt, H. U. (2004). Effects of sensory deprivation on columnar organization of neuronal circuits in the rat barrel cortex. *Eur J Neurosci* **20**, 1118-1124.

### Recordings from cardiac cells

- ❑ Bollensdorff, C., Knopp, A., Biskup, C., Zimmer, T., & Benndorf, K. (2004). Na<sup>+</sup> current through KATP channels: consequences for Na<sup>+</sup> and K<sup>+</sup> fluxes during early myocardial ischemia. *Am.J.Physiol Heart Circ.Physiol* **286**, H283-H295.
- ❑ Linz, K. and Meyer, R. (1997) Modulation of L-type calcium current by internal potassium in guinea pig ventricular myocytes. *Cardiovascular Research* **33**, 110-122.
- ❑ Lu, J., Dalton IV, J. F., Stokes, D. R. and Calabrese, R. L. (1997). Functional role of Ca<sup>2+</sup> currents in graded and spike- synaptic transmission between leech heart interneurons. *J.Europhysiol.* **77**, 1779–1794.
- ❑ Müller, A. et. al. (1997). Increase in gap junction conductance by an antiarrhythmic peptide. *Europ.J.Pharmacol* **327**, 65-72.
- ❑ Müller, A. et. al. (1997). Actions of the antiarrhythmic peptide AAP10 on intracellular coupling. *Naunyn-Schmiedeberg's Arch. Pharmacol.* **356**, 76-82.
- ❑ Pillekamp, F., Reppel, M., Dinkelacker, V., Duan, Y., Jazmati, N., Bloch, W., Brockmeier, K., Hescheler, J., Fleischmann, B. K., & Koehling, R. (2005). Establishment and characterization of a mouse embryonic heart slice preparation. *Cell Physiol Biochem.* **16**, 127-132.
- ❑ Räcke, H. F. et al. (1994). Fosinoprilate prolongs the action potential: reduction of I<sub>K</sub> and enhancement of L-type calcium current in guinea pig ventricular myocytes. *Cardiovascular Research* **28**, 201-208.

**LTP / LDP /LTD Investigations**

- ❑ Azad, S. C., Monory, K., Marsicano, G., Cravatt, B. F., Lutz, B., Zieglgansberger, W., & Rammes, G. (2004). Circuitry for associative plasticity in the amygdala involves endocannabinoid signaling. *J Neurosci* **24**, 9953-9961.
- ❑ Blank, T., Nijholt, I., Eckart, K., and Spiess, J. (2002). Priming of long-term potentiation in mouse hippocampus by corticotropin-releasing factor and acute stress: implications for hippocampus-dependent learning. *J Neurosci* **22**, 3788-94.
- ❑ Blank, T., Nijholt, I., Grammatopoulos, D. K., Randevo, H. S., Hillhouse, E. W., & Spiess, J. (2003). Corticotropin-releasing factor receptors couple to multiple G-proteins to activate diverse intracellular signaling pathways in mouse hippocampus: role in neuronal excitability and associative learning. *J Neurosci*. **23**, 700-707.
- ❑ DeBock, F., Kurz, J., Azad, S. C., Parsons, C. G., Hapfelmeier, G., Zieglgansberger, W., & Rammes, G. (2003).  $\alpha 2$ -Adrenoreceptor activation inhibits LTP and LTD in the basolateral amygdala: involvement of  $G_{i/o}$ -protein-mediated modulation of  $Ca^{2+}$ -channels and inwardly rectifying  $K^+$ -channels in LTD. *Eur.J.Neurosci*. **17**, 1411–1424.
- ❑ Dodt, H., Eder, M., Frick, A., and Zieglgansberger, W. (1999). Precisely localized LTD in the neocortex revealed by infrared-guided laser stimulation. *Science* **286**, 110-113.
- ❑ Eder, M., Zieglgansberger, W., & Dodt, H. U. (2002). Neocortical long-term potentiation and long-term depression: site of expression investigated by infrared-guided laser stimulation. *J.Neurosci*. **22**, 7558-7568.
- ❑ Huang, K. P., Huang, F. L., Jager, T., Li, J., Reymann, K. G., & Balschun, D. (2004). Neurogranin/RC3 enhances long-term potentiation and learning by promoting calcium-mediated signaling. *J Neurosci* **24**, 10660-10669.
- ❑ Marsicano, G., Wotjak, C. T., Azad, S. C., Bisognok, T., Rammes, G., Casciok, M. C., Hermann, H., Tang, J., Hofmann, C., Zieglgansberger, W., Di Marzok, V. & Lutz, B. (2002). The endogenous cannabinoid system controls extinction of aversive memories. *Nature* **418**, 530-533.
- ❑ Nakazawa K., Quirk, M. C., Chitwood, R. A., Watanabe, M., Yeckel, M. F., Sun, L. D., Kato, A., Carr, C. A., Johnston, D., Wilson, M. A. & Tonegawa, M. A. (2002). Requirement for Hippocampal CA3 NMDA Receptors in Associative Memory Recall. *Science* **297**, 211-218.
- ❑ Rammes, G., Palmer, M., Eder, M., Dodt, H. U., Zieglgansberger, W., & Collingridge, G. L. (2003). Activation of mGlu receptors induces LTD without affecting postsynaptic sensitivity of CA1 neurons in rat hippocampal slices. *J Physiol* **546**, 455-460.
- ❑ Rammes, G., Steckler, T., Kresse, A., Schutz, G., Zieglgansberger, W., and Lutz, B. (2000). Synaptic plasticity in the basolateral amygdala in transgenic mice expressing dominant-negative cAMP response element-binding protein (CREB) in forebrain. *Eur.J.Neurosci*. **12**, 2534-2546.
- ❑ Seeger, T., Fedorova, I., Zheng, F., Miyakawa, T., Koustova, E., Gomeza, J., Basile, A. S., Alzheimer, C., & Wess, J. (2004). M2 muscarinic acetylcholine receptor knock-out mice show deficits in behavioral flexibility, working memory, and hippocampal plasticity. *J Neurosci* **24**, 10117-10127.
- ❑ Wang, J., Yeckel, M. F., Johnston, D., & Zucker, R. S. (2004). Photolysis of Postsynaptic Caged  $Ca^{2+}$  Can Potentiate and Depress Mossy Fiber Synaptic Responses in Rat Hippocampal CA3 Pyramidal Neurons. *Journal of Neurophysiology* **91**, 1596-1607.
- ❑ Yeckel, M. F., Kapur, A., & Johnston, D. (1999). Multiple forms of LTP in hippocampal CA3 neurons use a common postsynaptic mechanism. *Nat.Neurosci*. **2**, 625-633.

### Performance test with active cell model

- ❑ Draguhn, A., Pfeiffer, M., Heinemann, U. and Polder, H. R. (1997). A simple hardware model for the direct observation of voltage-clamp performance under realistic conditions. *J.Neurosci.Meth.* **78**, 105-113.

### Intra- and extracellular low noise recording

- ❑ DeBock, F., Kurz, J., Azad, S. C., Parsons, C. G., Hapfelmeier, G., Zieglgänsberger, W., & Rammes, G. (2003).  $\alpha 2$ -Adrenoreceptor activation inhibits LTP and LTD in the basolateral amygdala: involvement of  $G_{i/o}$ -protein-mediated modulation of  $Ca^{2+}$ -channels and inwardly rectifying  $K^+$ -channels in LTD. *Eur.J.Neurosci.* **17**, 1411–1424.
- ❑ Kukley, M., Stausberg, P., Adelman, G., Chessell, I. P., & Dietrich, D. (2004). Ecto-nucleotidases and nucleoside transporters mediate activation of adenosine receptors on hippocampal mossy fibers by P2X7 receptor agonist 2'-3'-O-(4-benzoylbenzoyl)-ATP. *J Neurosci* **24**, 7128-7139.
- ❑ Lavin, A., Nogueira, L., Lapish, C. C., Wightman, R. M., Phillips, P. E., & Seamans, J. K. (2005). Mesocortical dopamine neurons operate in distinct temporal domains using multimodal signaling. *J Neurosci.* **25**, 5013-5023.
- ❑ Leger, J. F., Stern, E. A., Aertsen, A., & Heck, D. (2004). Synaptic Integration in Rat Frontal Cortex Shaped by Network Activity. *Journal of Neurophysiology.* **93**, 281-293.
- ❑ Seiffert, E., Dreier, J. P., Ivens, S., Bechmann, I., Tomkins, O., Heinemann, U., & Friedman, A. (2004). Lasting blood-brain barrier disruption induces epileptic focus in the rat somatosensory cortex. *J Neurosci* **24**, 7829-7836.
- ❑ Sillaber, I., Rammes, G., Zimmermann, S., Mahal, B., Zieglgänsberger, W., Wurst, W., Holsboer, F. & Spanagel, R. (2002). Enhanced and Delayed Stress-Induced Alcohol Drinking in Mice Lacking Functional CRH1 Receptors. *Science* **296**, 931-933.
- ❑ Strauss, U., Kole, M. H., Brauer, A. U., Pahnke, J., Bajorat, R., Rolfs, A., Nitsch, R., & Deisz, R. A. (2004). An impaired neocortical I is associated with enhanced excitability and absence epilepsy. *Eur.J Neurosci.* **19**, 3048-3058.
- ❑ Weiss, T., Veh, R. W., & Heinemann, U. (2003). Dopamine depresses cholinergic oscillatory network activity in rat hippocampus. *Eur.J Neurosci.* **18**, 2573-2580.

### Perforated Patch

- ❑ Hanganu, I. L., Kilb, W., & Luhmann, H. J. (2002). Functional synaptic projections onto subplate neurons in neonatal rat somatosensory cortex. *J.Neurosci.* **22**, 7165-7176.
- ❑ Hayashida, Y., Partida, G. J., & Ishida, A. T. (2004). Dissociation of retinal ganglion cells without enzymes. *J Neurosci.Methods* **137**, 25-35.
- ❑ Hayashida, Y. & Ishida, A. T. (2004). Dopamine receptor activation can reduce voltage-gated  $Na^+$  current by modulating both entry into and recovery from inactivation. *Journal of Neurophysiology* **92**, 3134-3141.
- ❑ Inceoglu, A. B., Hayashida, Y., Lango, J., Ishida, A. T., & Hammock, B. D. (2002). A single charged surface residue modifies the activity of iktotoxin, a beta-type  $Na^+$  channel toxin from *Parabuthus transvaalicus*. *Eur.J Biochem.* **269**, 5369-5376.
- ❑ Yanovsky, Y., Zhang, W., & Misgeld, U. (2005). Two pathways for the activation of small-conductance potassium channels in neurons of substantia nigra pars reticulata. *Neuroscience* **136**, 1027-1036.

---

**Recordings from Crustacea**

- ❑ DiCaprio, R. A. (2003). Nonspiking and Spiking Proprioceptors in the Crab: Nonlinear Analysis of Nonspiking TCMRO Afferents. *J Neurophysiol.* **89**, 1826-1836.
- ❑ DiCaprio, R. A. (2004). Information Transfer Rate of Nonspiking Afferent Neurons in the Crab. *Journal of Neurophysiology* **92**, 302-310.
- ❑ Gamble, E. R. & DiCaprio, R. A. (2003). Nonspiking and Spiking Proprioceptors in the Crab: White Noise Analysis of Spiking CB-Chordotonal Organ Afferents. *J Neurophysiol.* **89**, 1815-1825.
- ❑ Stein, W., Eberle, C. C., & Hedrich, U. B. S. (2005). Motor pattern selection by nitric oxide in the stomatogastric nervous system of the crab. *European Journal of Neuroscience* **21**, 2767-2781.

**Recordings from plant cells**

- ❑ Raschke, K. (2003). Alternation of the slow with the quick anion conductance in whole guard cells effected by external malate. *Planta* **217**, 651-657.
- ❑ Raschke, K., Shabahang, M., & Wolf, R. (2003). The slow and the quick anion conductance in whole guard cells: their voltage-dependent alternation, and the modulation of their activities. *Planta* **217**, 639-650.

**SEC-03 recordings**

- ❑ Martin-Pena, A., Acebes, A., Rodriguez, J. R., Sorribes, A., de Polavieja, G. G., Fernandez-Funez, P., & Ferrus, A. (2006). Age-independent synaptogenesis by phosphoinositide 3 kinase. *J Neurosci.* **26**, 10199-10208.

**Extracellular recordings (SEC-EXT)**

- ❑ Beckers, U., Egelhaaf, M., & Kurtz, R. (2007). Synapses in the fly motion-vision pathway: evidence for a broad range of signal amplitudes and dynamics. *J Neurophysiol.* **97**, 2032-2041.

**Other**

- ❑ Akay, T., Haehn, S., Schmitz, J., & Buschges, A. (2004). Signals From Load Sensors Underlie Interjoint Coordination During Stepping Movements of the Stick Insect Leg. *Journal of Neurophysiology* **92**, 42-51.
- ❑ Albrecht, J., Hanganu, I. L., Heck, N., & Luhmann, H. J. (2005). Oxygen and glucose deprivation induces major dysfunction in the somatosensory cortex of the newborn rat. *Eur.J Neurosci.* **22**, 2295-2305.
- ❑ Balasubramanyan, S., Stemkowski, P. L., Stebbing, M. J., & Smith, P. A. (2006). Sciatic Chronic Constriction Injury Produces Cell-type Specific Changes in the Electrophysiological Properties of Rat Substantia Gelatinosa Neurons. *J Neurophysiol.*
- ❑ Bickmeyer, U., Heine, M., Manzke, T., & Richter, D. W. (2002). Differential modulation of Ih by 5-HT receptors in mouse CA1 hippocampal neurons. *Eur.J.Neurosci.* **16**, 209-218.
- ❑ Bucher, D., Akay, T., DiCaprio, R. A., & Buschges, A. (2003). Interjoint coordination in the stick insect leg-control system: the role of positional signaling. *J Neurophysiol.* **89** , 1245-1255.
- ❑ Cornil, C. A., Balthazart, J., Motte, P., Massotte, L., & Seutin, V. (2002). Dopamine activates noradrenergic receptors in the preoptic area. *J Neurosci.* **22**, 9320-9330.

- 
- ❑ Daw, M. I., Bannister, N. V., & Isaac, J. T. (2006). Rapid, activity-dependent plasticity in timing precision in neonatal barrel cortex. *J Neurosci.* **26**, 4178-4187.
  - ❑ Dong, Y., Nasif, F. J., Tsui, J. J., Ju, W. Y., Cooper, D. C., Hu, X. T., Malenka, R. C., & White, F. J. (2005). Cocaine-induced plasticity of intrinsic membrane properties in prefrontal cortex pyramidal neurons: adaptations in potassium currents. *Journal of Neuroscience* **25**, 936-940.
  - ❑ Farrow, K., Haag, J., & Borst, A. (2003). Input organization of multifunctional motion-sensitive neurons in the blowfly. *J Neurosci.* **23**, 9805-9811.
  - ❑ Farrow, K., Borst, A., & Haag, J. (2005). Sharing receptive fields with your neighbors: tuning the vertical system cells to wide field motion. *Journal of Neuroscience* **25**, 3985-3993.
  - ❑ Gabbiani, F., Krapp, H. G., Koch, C., & Laurent, G. (2002). Multiplicative computation in a visual neuron sensitive to looming. *Nature* **420**, 320-324.
  - ❑ Gabriel, J. P., Scharstein, H., Schmidt, J., & Buschges, A. (2003). Control of flexor motoneuron activity during single leg walking of the stick insect on an electronically controlled treadmill. *J Neurobiol.* **56**, 237-251.
  - ❑ Gingl, E. & French, A. S. (2003). Active signal conduction through the sensory dendrite of a spider mechanoreceptor neuron. *J Neurosci.* **23**, 6096-6101.
  - ❑ Gingl, E., French, A. S., Panek, I., Meisner, S., & Torkkeli, P. H. (2004). Dendritic excitability and localization of GABA-mediated inhibition in spider mechanoreceptor neurons. *European Journal of Neuroscience* **20**, 59-65.
  - ❑ Grass, D., Pawlowski, P. G., Hirrlinger, J., Papadopoulos, N., Richter, D. W., Kirchhoff, F., & Hulsmann, S. (2004). Diversity of functional astroglial properties in the respiratory network. *J Neurosci.* **24**, 1358-1365.
  - ❑ Hadjilambrea, G., Mix, E., Rolfs, A., Muller, J., & Strauss, U. (2005). Neuromodulation by a Cytokine: Interferon- $\beta$  Differentially Augments Neocortical Neuronal Activity and Excitability. *Journal of Neurophysiology* **93**, 843-852.
  - ❑ Hepp, S., Gerich, F. J., & Mueller, M. (2005). Sulfhydryl Oxidation Reduces Hippocampal Susceptibility To Hypoxia-Induced Spreading Depression By Activating BK-Channels. *Journal of Neurophysiology* 00291.
  - ❑ Hoger, U., Torkkeli, P. H., & French, A. S. (2005). Calcium concentration changes during sensory transduction in spider mechanoreceptor neurons. *European Journal of Neuroscience* **22**, 3171-3178.
  - ❑ Hu, X. T., Basu, S., & White, F. J. (2004). Repeated Cocaine Administration Suppresses HVA-Ca<sup>2+</sup> Potentials and Enhances Activity of K<sup>+</sup> Channels in Rat Nucleus Accumbens Neurons. *Journal of Neurophysiology* **92**, 1597-1607.
  - ❑ Jiang, Z. G., Nuttall, A. L., Zhao, H., Dai, C. F., Guan, B. C., Si, J. Q., & Yang, Y. Q. (2005). Electrical coupling and release of K<sup>+</sup> from endothelial cells co-mediate ACh-induced smooth muscle hyperpolarization in inner ear artery. *J. Physiol.* **564**, 475-487.
  - ❑ Juusola, M. and Hardie, R. C. (2001). Light Adaptation in *Drosophila* Photoreceptors: I. Response Dynamics and Signaling Efficiency at 25° C. *J.Gen.Physiol.* **117**, 3-25.
  - ❑ Juusola, M. and Hardie, R. C. (2001). Light Adaptation in *Drosophila* Photoreceptors: II. Rising Temperature Increases the Bandwidth of Reliable Signaling, *J.Gen.Physiol.* **117**, 27-41.
  - ❑ Juusola, M., Niven, J. E., & French, A. S. (2003). Shaker k<sup>+</sup> channels contribute early nonlinear amplification to the light response in *Drosophila* photoreceptors. *J Neurophysiol.* **90**, 2014-2021.

- 
- ❑ Kohling, R., Koch, U. R., Hamann, M., & Richter, A. (2004). Increased excitability in cortico-striatal synaptic pathway in a model of paroxysmal dystonia. *Neurobiol.Dis.* **16**, 236-245.
  - ❑ Ludwar, B. C., Westmark, S., Buschges, A., & Schmidt, J. (2005). Modulation of membrane potential in mesothoracic moto- and interneurons during stick insect front-leg walking. *Journal of Neurophysiology* **94**, 2772-2784.
  - ❑ Leger, J. F., Stern, E. A., Aertsen, A., & Heck, D. (2005). Synaptic integration in rat frontal cortex shaped by network activity. *Journal of Neurophysiology* **93**, 281-293.
  - ❑ Marsicano, G., Goodenough, S., Monory, K., Hermann, H., Eder, M., Cannich, A., Azad, S. C., Cascio, M. G., Gutierrez, S. O., van der, S. M., Lopez-Rodriguez, M. L., Casanova, E., Schutz, G., Zieglgansberger, W., Di, M., V, Behl, C., & Lutz, B. (2003). CB1 cannabinoid receptors and on-demand defense against excitotoxicity. *Science* **302**, 84-88.
  - ❑ Manzke, T., Guenther, U., Ponimaskin, E. G., Haller, M., Dutschmann, M., Schwarzacher, S., & Richter, D. W. (2003). 5-HT<sub>4</sub>(a) receptors avert opioid-induced breathing depression without loss of analgesia. *Science* **301**, 226-229.
  - ❑ Mentel, T., Krause, A., Pabst, M., El Manira, A., & Buschges, A. (2006). Activity of fin muscles and fin motoneurons during swimming motor pattern in the lamprey. *Eur.J Neurosci.* **23**, 2012-2026.
  - ❑ Muller, A., Kukley, M., Stausberg, P., Beck, H., Muller, W., & Dietrich, D. (2005). Endogenous Ca<sup>2+</sup> Buffer Concentration and Ca<sup>2+</sup> Microdomains in Hippocampal Neurons. *Journal of Neuroscience* **25**, 558-565.
  - ❑ Naro, F., De, A., V, Coletti, D., Molinaro, M., Zani, B., Vassanelli, S., Reggiani, C., Teti, A., & Adamo, S. (2003). Increase in cytosolic Ca<sup>2+</sup> induced by elevation of extracellular Ca<sup>2+</sup> in skeletal myogenic cells. *Am.J.Physiol Cell Physiol* **284**, C969-C976.
  - ❑ Nasif, F. J., Sidiropoulou, K., Hu, X. T., & White, F. J. (2005). Repeated cocaine administration increases membrane excitability of pyramidal neurons in the rat medial prefrontal cortex. *J.Pharmacol.Exp.Ther.* **312**, 1305-1313.
  - ❑ Okabe, A., Kilb, W., Shimizu-Okabe, C., Hanganu, I. L., Fukuda, A., & Luhmann, H. J. (2004). Homogenous glycine receptor expression in cortical plate neurons and cajal-retzius cells of neonatal rat cerebral cortex. *Neuroscience* **123**, 715-724.
  - ❑ Panek, I., French, A. S., Seyfarth, E. A., Sekizawa, S. I., & Torkkeli, P. H. (2002). Peripheral GABAergic inhibition of spider mechanosensory afferents. *Eur.J.Neurosci.* **16**, 96-104.
  - ❑ Pangrsic, T., Stusek, P., Belusic, G., & Zupancic, G. (2005). Light dependence of oxygen consumption by blowfly eyes recorded with a magnetic diver balance. *J Comp Physiol A Neuroethol.Sens.Neural Behav.Physiol* **191**, 75-84.
  - ❑ Pascual, O., Traiffort, E., Baker, D. P., Galdes, A., Ruat, M., & Champagnat, J. (2005). Sonic hedgehog signalling in neurons of adult ventrolateral nucleus tractus solitarius. *Eur.J Neurosci.* **22**, 389-396.
  - ❑ Pomper, J. K., Haack, S., Petzold, G. C., Buchheim, K., Gabriel, S., Hoffmann, U., & Heinemann, U. (2005). Repetitive Spreading Depression-Like Events Result in Cell Damage in Juvenile Hippocampal Slice Cultures Maintained in Normoxia. *Journal of Neurophysiology*.
  - ❑ Ranft, A., Kurz, J., Deuringer, M., Haseneder, R., Dodt, H. U., Zieglgansberger, W., Kochs, E., Eder, M., & Hapfelmeier, G. (2004). Isoflurane modulates glutamatergic and GABAergic neurotransmission in the amygdala. *Eur J Neurosci* **20**, 1276-1280.
  - ❑ Rastan, A. J., Walther, T., Kostelka, M., Garbade, J., Schubert, A., Stein, A., Dhein, S., & Mohr, F. W. (2005). Morphological, electrophysiological and coupling characteristics of

- bone marrow-derived mononuclear cells--an in vitro-model. *European Journal of Cardio-Thoracic Surgery* **27**, 104-110.
- ❑ Reiprich, P., Kilb, W., & Luhmann, H. J. (2005). Neonatal NMDA Receptor Blockade Disturbs Neuronal Migration in Rat Somatosensory Cortex In Vivo. *Cerebral Cortex* **15**, 349-358.
  - ❑ Ren, J., Lee, S., Pagliardini, S., Gerard, M., Stewart, C. L., Greer, J. J., & Wevrick, R. (2003). Absence of Ndn, encoding the Prader-Willi syndrome-deleted gene necdin, results in congenital deficiency of central respiratory drive in neonatal mice. *J Neurosci.* **23**, 1569-1573.
  - ❑ Ren, J. & Greer, J. J. (2006). Modulation of respiratory rhythmogenesis by chloride-mediated conductances during the perinatal period. *J Neurosci.* **26**, 3721-3730.
  - ❑ Sacchi, O., Rossi, M. L., Canella, R., & Fesce, R. (2006). Synaptic and somatic effects of axotomy in the intact, innervated rat sympathetic neuron. *J Neurophysiol.* **95**, 2832-2844.
  - ❑ Stett, A., Bucher, V., Burkhardt, C., Weber, U., & Nisch, W. (2003). Patch-clamping of primary cardiac cells with micro-openings in polyimide films. *Med.Biol.Eng Comput.* **41**, 233-240.
  - ❑ Salgado, V. L. & Saar, R. (2004). Desensitizing and non-desensitizing subtypes of alpha-bungarotoxin-sensitive nicotinic acetylcholine receptors in cockroach neurons. *J Insect Physiol* **50**, 867-879.
  - ❑ Torkkeli, P. H., Sekizawa, Ss. and French, A. S. (2001). Inactivation of voltage-activated Na<sup>+</sup> currents contributes to different adaptation properties of paired mechanosensory neurons. *J.Neurophysiol* **85**, 1595–1602.
  - ❑ Torkkeli, P. H. and French, A. S. (2001). Simulation of Different Firing Patterns in Paired Spider Mechanoreceptor Neurons: The Role of Na Channel Inactivation, *J.Neurophysiol.* **87**, 1363–1368.
  - ❑ Vahasoyrinki, M., Niven, J. E., Hardie, R. C., Weckstrom, M., & Juusola, M. (2006). Robustness of neural coding in Drosophila photoreceptors in the absence of slow delayed rectifier K<sup>+</sup> channels. *J Neurosci.* **26**, 2652-2660.
  - ❑ Vassanelli, S. and Fromherz, P. (1999). Transistor Probes Local Potassium Conductances in the Adhesion Region of Cultured Rat Hippocampal Neurons. *J.Neurosci* **19** (16), 6767–6773.
  - ❑ Wang, J., Yeckel, M. F., Johnston, D., & Zucker, R. S. (2004). Photolysis of postsynaptic caged Ca<sup>2+</sup> can potentiate and depress mossy fiber synaptic responses in rat hippocampal CA3 pyramidal neurons. *Journal of Neurophysiology* **91**, 1596-1607.
  - ❑ Wolfram, V. & Juusola, M. (2004). The Impact of Rearing Conditions and Short-Term Light Exposure on Signaling Performance in Drosophila Photoreceptors. *Journal of Neurophysiology* **92**, 1918-1927.

### 13.2. Books

- ❑ Boulton, A.A., Baker, G.B. and Vanderwolf, C.H. (eds.) (1990) Neurophysiological techniques. Basic methods and concepts. Humana Press, Clifton, New Jersey.
- ❑ Cole, K.S. (1968) Membranes ions and impulses. University of California Press, Berkely, CA.
- ❑ Ferreira, H.G. and Marshall, M.W. (1985) The biophysical basis of excitability. Cambridge University Press, Cambridge.
- ❑ Fröhr, F. (1985) Electronic control engineering made easy. An introduction for beginners. Siemens AG, Berlin and Munich.
- ❑ Horowitz, P. and Hill, W. (1989) The art of electronics. Cambridge University Press, NY
- ❑ Jack, J.J.B., Noble, D. and Tsien, R.W. (1975) Electric current flow in excitable cells. Clarendon Press, Oxford.
- ❑ Kettenmann, H. and Grantyn, R. (eds.) (1992) Practical electrophysiological methods. Wiley-Liss, New York.
- ❑ Neher, E. (1974) Elektrische Meßtechnik in der Physiologie. Springer-Verlag, Berlin.
- ❑ Numberger, M. and Draguhn, A. (eds.) (1996) Patch-Clamp-Technik. Spektrum Akad. Verl., Heidelberg, Berlin, Oxford.
- ❑ Ogden, D.C. (ed.) (1994) Microelectrode techniques. The Plymouth Workshop Handbook. 2nd edition, The Company of Biologists Limited, Cambridge.
- ❑ Polder, H.R. (1984) Entwurf und Aufbau eines Gerätes zur Untersuchung der Membranleitfähigkeit von Nervenzellen und deren Nichtlinearität nach der potentiostatischen Methode (Voltage-Clamp-Methode) mittels einer Mikroelektrode. Diplomarbeit, Technische Universität München.
- ❑ Rudy, B. and Iverson, L.E. (eds.) (1992) Ion channels. In: Methods in enzymology. Vol. 207, Academic Press, San Diego, CA, USA.
- ❑ Sahn III, W.H. and Smith, M.W. (eds.) (1984) Optoelectronics manual. 3rd edition, General Electric Company, Auburn, NY, USA.
- ❑ Sakmann, B. and Neher, E. (eds.) (1995) Single channel recording. 2nd Edition, Plenum.NY,.
- ❑ Smith, T.G., Jr., Lecar, H., Redmann, S.J. and Gage, P.W. (eds.) (1985) Voltage and patch clamping with microelectrodes. American Physiological Society, Bethesda; The Williams & Wilkins Company, Baltimore.
- ❑ Windhorst, U. and H. Johansson (eds.) Modern Techniques in Neuroscience Research, Springer, Berlin, Heidelberg, New York, 1999

## 14. SEC-03M Specifications – Technical Data

### MODES OF OPERATION

VC:	Voltage Clamp mode (discontinuous)
CC:	Current Clamp mode (discontinuous)
OFF:	Current- and Voltage Clamp disabled
BR:	Bridge Mode (continuous CC)
EXT:	External control mode; the mode of operation can be set by a TTL pulse applied to the MODE SELECT BNC.
MODE selection:	toggle switch, LED indicators; remote selection by TTL pulse

### HEADSTAGES

#### **Standard headstage**

Operation voltage:	$\pm 15$ V
Input resistance:	$<10^{13}$ $\Omega$ (internally adjustable)
Current range (continuous mode):	120 nA into 100 M $\Omega$
CC control:	Coarse control for input capacity compensation
Electrode connector:	gold plated SUBCLIC (SMB) with driven shield
Driven shield output:	2.3 mm connector, range $\pm 15$ V, impedance 250 $\Omega$
Ground:	2.3 mm connector or headstage enclosure
Holding bar:	diameter 8 mm, length 100 mm
Size:	100x40x25 mm
Headstage enclosure is connected to ground	

#### **Low-noise (whole-cell) headstage (SEC-HSP)**

Operation voltage:	$\pm 15$ V
Input resistance:	$<10^{13}$ $\Omega$ (internally adjustable)
Current range (continuous mode):	12 nA into 100 M $\Omega$
external CC control:	Coarse control for input capacity compensation
Electrode connector:	BNC connector with driven shield
Driven shield output:	1 mm connector, range $\pm 15$ V, impedance 250 $\Omega$
Ground:	1 mm connector or headstage enclosure
Mounting plate:	60x50 mm with four 6 mm holes
Headstage enclosure is connected to ground	

#### **Differential input headstage (SEC-HSD)**

Operation voltage:	$\pm 15$ V
Input resistance:	$<10^{13}$ $\Omega$ (internally adjustable)
CMR:	$>90$ dB
Current range (continuous mode):	120 nA into 100 M $\Omega$
CC control:	Coarse control for input capacity compensation
Electrode connectors:	two gold plated SUBCLIC (SMB) with driven shields
Driven shield output:	2.3 mm connector, range $\pm 15$ V, impedance 250 $\Omega$
Ground:	2.3 mm connector or headstage enclosure
Holding bar:	diameter 8 mm, length 100 mm
Size:	100x40x25 mm
Headstage enclosure is connected to ground	

ELECTRODE PARAMETER CONTROLS

Offset: ten-turn control,  $\pm 200$  mV  
 Capacity compensation: range 0-30 pF  
 adapts compensation circuit to electrode parameters  
 coarse control at headstage  
 fine control at front panel: ten-turn potentiometer

BANDWIDTH and SPEED OF RESPONSE

Full power bandwidth ( $R_{EL} = 0$ ):  $> 100$  kHz  
 Rise time (10-90%,  $R_{EL} = 100$  M $\Omega$ ):  $< 30$   $\mu$ s  
 Rise time (10-90%,  $R_{EL} = 5$  M $\Omega$ ):  $< 8$   $\mu$ s  
 Electrode artifact decay  
 (switched modes, 10 nA signal):  $< 1$   $\mu$ s ( $R_{EL} = 5$  M $\Omega$ );  $< 1.5$   $\mu$ s ( $R_{EL} = 100$  M $\Omega$ )  
 CAPACITY COMPENSATION tuned with no overshoot.

ELECTRODE RESISTANCE TEST

obtained by application of square current pulses  $\pm 1$  nA; 10 mV/M $\Omega$ ; display XXX M $\Omega$

SWITCHED MODES PARAMETERS

Switching frequency: linear control, 2-40 kHz; duty cycle: fixed to  $\frac{1}{4}$  (25% current injection)

CURRENT RANGE in SWITCHED MODE

Standard headstage:  $\pm 30$  nA  
 SEC-HSP headstage:  $\pm 3$  nA

SWITCHED MODE OUTPUTS

Electrode potential: max.  $\pm 12$  V, output impedance: 250  $\Omega$   
 Switching frequency: TTL, output impedance: 250  $\Omega$

CURRENT OUTPUT

10 nA / V; output impedance: 250  $\Omega$ ; current display: X.XX nA

POTENTIAL OUTPUT

Sensitivity: x10 mV; output impedance: 250  $\Omega$ ; potential display: XXX mV

CURRENT CLAMP

Input: 1 nA/V; input resistance:  $> 100$  k $\Omega$   
 HOLD: X.XX nA ten-turn digital control with -/0/+ switch, max. 10 nA  
 BRIDGE balance: XXX M $\Omega$  with ten-turn digital control  
 Noise (BRIDGE MODE): 400  $\mu$  V<sub>pp</sub> / pA<sub>pp</sub> with 100 M $\Omega$  resistance at 10 kHz bandwidth

VOLTAGE CLAMP

Input: /10 mV; input resistance  $> 100$  k $\Omega$   
 HOLD: XXX mV, ten-turn digital control with +/0/- switch, max. 1000 mV  
 GAIN: 100 nA/V - 10  $\mu$ A/V ten-turn linear control  
 Noise: potential output:  $< 400$   $\mu$  V<sub>pp</sub>, current output:  $< 400$  pA<sub>pp</sub>.

SPEED of RESPONSE (VC Mode)

1 % settling time: <80  $\mu$ s for 10 mV step and <800  $\mu$ s for 50 mV step applied to a cell model  
( $R_{EL} = 100 \text{ M}\Omega$ ,  $R_m = 50 \text{ M}\Omega$ ,  $C_m = 470 \text{ pF}$ , duty cycle = 25%, switching frequency = 30 kHz, standard headstage)

DIMENSIONS

Front panel: 24 HP (121.5 mm) x 3U (128.5 mm)

Housing: 7" (175 mm) deep

EPMS-07 system

POWER REQUIREMENTS:

115/230 V AC, 60/50 Hz, fuse 2 A / 1 A, slow, 45-60 W (depending on the modules plugged in)

DIMENSIONS:

19" rackmount cabinet, 3U high (1U = 1 3/4" = 44.45 mm)

## 15. Index

- abbreviations 4
- Absolute value optimum 51
- accessories 13
- AVO-method 51
- basic installation 22
- basic settings 22
- bias current adjustment 27
- BIAS current potentiometer 15
- bridge balance 29, 30, 42
- BRIDGE BALANCE potentiometer 15
- C. COMP. potentiometer 19
- cell model 23
  - connections and operation 24, 25
  - description 23
- clamp performance 50
- closed loop system 49
- control theory 49
- CUR.STIM. INPUT connector 16
- CURRENT display 15
- CURRENT OUTPUT connector 17
- ELECT. POTENTIAL connector 17
- electrical connections 22
- electrode 28
  - artifacts 43
  - capacity compensation 31
  - offset compensation 28
  - selection 28
- GAIN potentiometer 19
- HEADSTAGE connector 17
- Headstages 19
- HOLD. POT. (mV) potentiometer 18
- HOLD.CUR.(nA) potentiometer 16
- INTEGR. (ms) potentiometer 18
- Linear optimum 51
- LO-method 51
- MODE OF OPERATION LEDs 15
- MODE OF OPERATION switch 15
- MODE SELECT connector 18
- model circuit sharp electrode 9, 41
- model circuit suction (patch) electrode 9
- modulus hugging 49
- OFFSET potentiometer 15
- operation modes
  - testing 39
- PI-controllers 49
- POTENTIAL / RESISTANCE display 15
- POTENTIAL OUTPUT connector 18
- REL push button 19
- sample experiments 41
  - sharp electrode 41
  - suction (patch) electrode 44
- sealing 45
- Selection of the switching frequency 31
- sharp electrode 41
- sharp electrodes 9
- SO-method 51
- Speed of Response 50
- suction electrodes 44
- SW.FREQ. (kHz) potentiometer 16
- SWITCH. FREQUENCY (SYNC.OUT) connector 17
- Symmetrical optimum 51
- SYNC. / INTERN switch 16
- testing 27
- Trouble Shooting 48
- tuning 27
- VC optimization methods 46
- VOLTAGE COMMAND INPUT connector 18